ELSEVIER

Institut Pasteur

Microbes and Infection 16 (2014) 320–327

www.elsevier.com/locate/micinf

Original article

Cross-reactivity analysis of T cell receptors specific for overlapping HIV-1 Nef epitopes of different lengths

Chihiro Motozono [a,1], Masaru Yokoyama [b], Hironori Sato [b], Takamasa Ueno [a,*]

[a] *Center for AIDS Research, Kumamoto University, Kumamoto, Japan*
[b] *Laboratory of Viral Genomics, Pathogen Genomics Center, National Institute of Infectious Diseases, Tokyo, Japan*

Received 1 November 2013; accepted 22 December 2013
Available online 28 December 2013

Abstract

Overlapping peptides of different lengths from a certain immunodominant region can be presented by the same HLA class I molecule and elicit different T cell responses. However, how peptide-length specificity of antigen-specific $CD8^+$ T lymphocytes influence cross-reactivity profiles of these cells remains elusive. This question is particularly important in the face of highly variable pathogens such as HIV-1. Here, we examined this problem by using HLA-B*35:01-restricted $CD8^+$ T lymphocytes specific for Nef epitopes, i.e., RY11 (RPQVPLRPMTY), VY8 (VPLRPMTY), and RM9 (RPQVPLRPM), in which VY8 and RM9 were contained entirely within RY11, in combination with a T cell receptor (TCR) reconstruction system as well as HLA-B35 tetramers and a set of a single-variant peptide library. The TCR reactivity toward the peptide-length variants was classified into three types: mutually exclusive specificity toward (1) RY11 or (2) VY8 and (3) cross-recognition toward RM9 and RY11. TCR cross-reactivity toward variant peptides was similar within the same peptide-length reactivity type but was markedly different between the types. Thus, TCRs showing similar peptide-length reactivity have shared peptide recognition footprints and thereby similar weakness to antigenic variations, providing us with further insight into the antiviral vaccine design.

Keywords: HIV-1; $CD8^+$ T cell; TCR; Antigenic peptide; Cross-reactivity; HLA-B*35:01

1. Introduction

HLA class I (HLA-I) molecules form a highly polymorphic antigen-binding cleft and play a central role in selection and presentation of antigenic peptides to T lymphocytes. Crystal structures of HLA-I in complex with an antigenic peptide have shown that the central residues in the peptide are generally exposed at the outside of the HLA binding groove, thus affording recognition by cognate T cell receptors (TCRs) [1]. The fixed anchors at the N- and C-termini of the antigenic peptide of 8-13 amino acids in length, and the closed conformation of the HLA-I groove, force longer peptides to bulge further out of the groove to accommodate the extra central peptide residues [2]. Such a difference in peptide conformation as well as the size of the central bulge bound to HLA substantially influences the TCR selection and recognition [3]. The same HLA-I molecule can eventually present various closely related overlapping peptides of different lengths [4], while closely related HLA-I allomorphs have different length preference toward overlapping epitopes in some settings that result in qualitatively variable T cell-mediated viral control [5–9].

Viruses such as the highly variable HIV-1 and hepatitis C viruses can mutate and thus escape from CTL responses [10,11], and it is becoming evident that CTLs with the capacity to cross-recognize naturally occurring viral variants are advantageous for viral control *in vivo* [12–17]. In a region of viral proteins where multiple overlapping epitopes of various length are clustering, a mutation results in a change in multiple

* Corresponding author. Center for AIDS Research, Kumamoto University, 2-2-1 Chuo-ku, Honjo, Kumamoto 860-0811, Japan. Tel.: +81 96 373 6826; fax: +81 96 373 6825.
E-mail address: uenotaka@kumamoto-u.ac.jp (T. Ueno).
[1] Present address: Department of Immunology, Kinki University School of Medicine, Osaka, Japan.

1286-4579/$ - see front matter © 2013 Institut Pasteur. Published by Elsevier Masson SAS. All rights reserved.
http://dx.doi.org/10.1016/j.micinf.2013.12.005

epitopes and may differentially influence T cell responses specific for such epitopes [5]. This case is likely where an HLA-I allomorph presents multiple overlapping epitopes of different length. However, how such overlapping peptides of different lengths presented by the same HLA allele affect length preference and cross-reactive potency of TCRs toward variant peptides remains unclear.

In HIV-1 Nef, a highly immunogeneic viral protein, a number of CTL epitopes are located within a multi-restricted, immunodominant central region spanning residues 73-94 and 113-147, including a highly conserved polyproline region at residues 73-82 [18,19]. In particular, HLA-B*35:01, which prefers proline at the second position of its bound peptides [19,20], can present multiple overlapping epitopes within this region, leading to elicitation of different antigen-specific CTL responses [5,6,19,20]. In fact, we previously reported that in HIV-infected patients with HLA-B*35:01, Nef protein elicited dominant CTL responses [21], with a short epitope (VY8; VPLRPMTY) and an amino-terminal extended long epitope (RY11; RPQVPLRPMTY) being different optimal epitopes presented by HLA-B*35:01 [5,6]. There is also another potential epitopic peptide sequence, RM9 (RPQVPLRPM), within RY11. In this present study, employing TCR-reconstructed T cells, we carefully investigated peptide-length preferences of various TCRs and examined whether, and if so how, cross-reactivity profiles of these TCRs were affected by peptide-length preference.

2. Materials and Methods

2.1. Reagents

HLA-B35 tetramers in complex with the RY11, RM9 or VY8 peptides were prepared as previously described [21]. Peptides were designed based on the subtype B consensus sequence of HIV-1 Nef (see Los Alamos database at http://www.hiv.lanl.gov/content/index) and were prepared by using an automated multiple peptide synthesizer. The purity and integrity of the synthesized peptides was examined by high-performance liquid chromatography and mass spectrometry, and the peptides with >90% purity were used in this study. Antibodies used were the following: PE-conjugated anti-mouse CD3ε mAb (2C11: BioLegend), anti-human CD8-PerCP (BD Biosciences), and anti-human CD3-FITC (DakoCytomation).

2.2. CTL clones

CTL clones that had been established by using PBMC samples taken from HLA-B*35:01$^+$ individuals (Pt-01, -03, -19, and -33) with an HIV-1 infection were used [5,6,21]. CTL clone H231 generated from PBMC from Pt-01 was designated CTL 01-H231, and other clones were similarly designated. Cytotoxic assays were done as previously described [5,6,21]. The study was conducted in accordance with the human experimentation guidelines of Kumamoto University.

2.3. TCR reconstruction

TCR-encoding genes of CTL clones were obtained by using a SMART PCR cDNA synthesis kit (Clontech, Palo Alto, CA) as described previously [22,23]. The resultant TCR αβ genes were separately cloned into a retrovirus vector pMX (provided by T. Kitamura at Tokyo University) and delivered into a TCR-deficient mouse T cell hybridoma cell line, TG40 (provided by T. Saito at RIKEN Institute), as previously described [6,22]. The human CD8α gene was similarly delivered into the cells as needed. TG40 cells transduced with TCR genes isolated from CTL 01-H231 were designated TG40-H231 and other TCR-transduced cells were similarly designated.

TCR recognition of cognate antigens was measured in terms of IL-2 secretion by TCR-transduced TG40 cells, as described earlier [6,22]. Unless otherwise specified, C1R cells expressing HLA-B*35:01 (C1R-B3501, 10^4 cells/well), TCR-transduced TG40 cells (2×10^4 cells/well), and peptides were mixed and incubated for 24 h at 37 °C. The resultant culture supernatant was then collected, and the amount of IL-2 was determined by analyzing the proliferative activity of the IL-2 indicator cell line CTLL-2.

2.4. Flow cytometric analysis

CTL clones were stained with PE- or allophycocyanin-labeled HLA-B35 tetramers at 37 °C for 15 min followed by incubation with anti-CD8-PerCP and anti-CD3-FITC at 4 °C for 15 min. By flow cytometry, CD3$^+$ CD8$^+$ live cells were gated and analyzed for tetramer binding, as described previously [6]. TCR-reconstructed TG40 cells were stained with HLA-B35 tetramers at 4 °C for 15 min followed by anti-CD3-PE at 4 °C for 20 min. By flow cytometry, CD3$^+$ live cells were gated and analyzed for tetramer binding as described earlier [6,22]. Cells were analyzed by use of a FACS Calibur or FACS Canto II flow cytometer (BD Biosciences), and the data were further analyzed by using Flow Jo (Treestar, San Diego CA).

2.5. Structural modeling of pMHC

The crystal structure of HLA-B*35:01 with the VY8 peptide at a resolution of 2.00 Å (PDB code: 1A1N [24]) was taken from the Protein Data Bank to construct the complexes between HLA-B*35:01 and RM9 or RY11. The modeling was performed by using tools available in the Molecular Operating Environment (MOE, MOE 2012.1001; Chemical Computing Group Inc., Montreal, Quebec, Canada) as follows: First, hydrogen was added to the HLA structure. The HLA-B*35:01 structure was thermodynamically optimized by energy minimization using MOE and an AMBER12EHT force field [25] combined with the generalized Born model of aqueous solvation implemented in MOE [26]. Next, the RM9 or RY11 peptide models on the HLA-B*35:01 structure were constructed by the homology modeling technique using 'MOE-Homology' in MOE. Finally, the RM9 or RY11 model was

docked with the HLA-B*35:01 structures by using the automated ligand docking program ASEDock [27] operated in MOE.

3. Results

3.1. Multiple overlapping epitopic sequences in Nef in the context of HLA-B*35:01

In the HLA-B*35:01-restricted epitopic peptide sequence RPQVPLRPMTY (RY11), located in the immunodominant central region of Nef (Fig. 1), there are two additional sequences, VPLRPMTY (VY8) and RPQVPLRPM (RM9), that have similar motifs for HLA-B*35:01 binding, i.e., Pro at position 2 (P2) and a hydrophobic residue at the C-terminus [19–21]. In fact, RY11 [21,28] and VY8 [5,29] have been reported as CTL epitopes presented by HLA-B*35:01, although RM9 is not yet known to be an HLA-B*35:01-restricted epitope. The results of an HLA-stabilization assay showed that RM9 bound to HLA-B*35:01 with a half maximal binding level (BL_{50}) of 22 μM, which is comparable to that of RY11 (23 μM) and VY8 (41 μM), suggesting that RM9 could also be presented by HLA-B*35:01 for TCR recognition. Corroboratively, the peptide replacement structural modeling studies showed that RM9 could be accommodated in the peptide-binding groove of HLA-B*35:01, as could RY11 and VY8 (Fig. 1). Also, VY8, RM9, and RY11 peptides each had a distinct surface area available for TCR binding (Fig. 1).

Because $CD8^+$ T lymphocytes have preference toward peptide-length variants [3,8,9,21,30,31], we tested again a panel of CTL clones (CTL01-H231, CTL03-G8, CTL19-27, CTL19-139, and CTL33-S1) for cytotoxic activity toward cells pulsed with VY8, RM9 or RY11 peptides. All CTL clones showed cytotoxic activity toward target cells pulsed with RY11 (Fig. 2A), suggesting that RY11 contained antigenic determinants recognized by all of these TCRs, which would be consistent with previous studies [6,21]. However, CTL19-139 and CTL33-S1 showed more potent activity toward cells pulsed with VY8 than with RY11 and no response toward cells pulsed with RM9 (Fig. 2A). In support of this finding, these clones showed binding exclusively to VY8/B35 tetramers and not to RM9/B35 or RY11/B35 tetramers (Fig. 2B), indicating that CTL19-139 and CTL33-S1 were exclusively specific for VY8. CTL01-H231 did not show cytotoxic activity toward cells pulsed with RM9 or VY8 (Fig. 2A). In fact, CTL01-H231 bound exclusively to RY11/B35 tetramers, but not to RM9/B35 or VY8/B35 ones (Fig. 2B), indicating that CTL01-H231 was exclusively specific for RY11. On the other hand, CTL03-G8 and CTL19-27 showed cytotoxic activity toward cells pulsed with both RM9 and RY11; although at a lower peptide concentration these clones showed about 10 times more potent activity toward RM9- than toward RY11-pulsed cells (Fig. 2A). Consistently, CTL03-G8 and CTL19-27 exhibited higher binding activity toward the RM9/B35 tetramer than toward the RY11/B35 one (Fig. 2B), suggesting that RM9 could be an epitope for these CTLs.

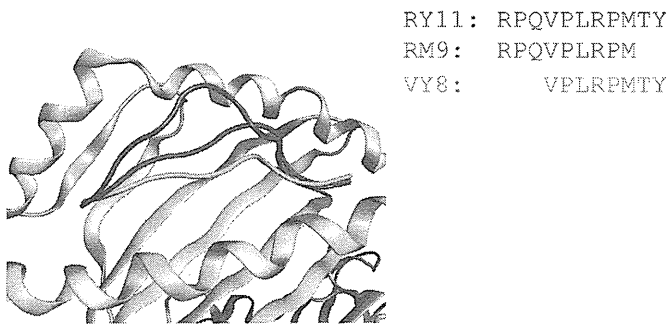

Fig. 1. Structural modeling of HLA-B*35:01 in complex with RY11, RM9 or VY8. The HLA-B*35:01-peptide complex models were constructed by using the crystal structures of HLA-B*35:01 in complex with VY8 at a resolution of 2.00 Å (PDB code: 1A1N [24]), as described in Materials and Methods. RY11 (blue) and RM9 (magenta) are superimposed on the VY8 (cyan) peptide-HLA-B*35:01 model.

3.2. Fine specificity analysis by use of TCR-reconstructed cells

To certify fine specificity and peptide-length preference of the above CTLs, TCRs isolated from these CTLs were reconstructed on TCR-deficient T cell line TG40 cells; because this method allowed us to precisely examine the TCR-peptide-MHC interaction without any influence of functional differences among primary CTLs [6,22,23]. By introduction of TCR genes into TG40 cells (designated TG40-H231, TG40-G8, TG40-27, TG40-139, and TG40-S1), TCR/CD3 expression was clearly observed in all cells (Fig. 3A), confirming TCR reconstruction on the TG40 cell surface. We next tested the TCR specificity by peptide titration and tetramer staining. We confirmed that TG40-139 and S1 efficiently recognized target cells pulsed with the VY8 peptide and bound to VY8/B35 tetramers (Fig. 3B and C), in good agreement with the CTL data shown in Fig. 2. As expected, TG40-H231 exclusively recognized target cells pulsed with RY11 (Fig. 3B) and bound to the RY11/B35 tetramer but not to the RM9/B35 tetramer (Fig. 3C). On the other hand, TG40-G8 and TG40-27 responded towards cells pulsed with both RM9 and RY11 without much difference in sensitivity in the peptide titration experiments (Fig. 3B); whereas both cells showed a different pattern of tetramer binding (Fig. 3C). TG40-G8 showed substantial binding activity toward RM9/B35 tetramers (Fig. 3C), but weak binding activity toward RY11/B35 ones (Fig. 3C). In contrast, TG40-27 showed extremely weak or virtually no binding to RY11/B35 or RM9/B35 tetramers (Fig. 3C), although CTL19-27 bound to both tetramers (Fig. 2B). Taken together, these data indicate that TCRs that favorably recognized RM9 also cross-recognized RY11 in the context of HLA-B*35:01, at least to some extent.

3.3. Cross-reactivity profiles of TCRs towards an array of variant peptides

We next analyzed TCR cross-reactivity towards 198 RY11-based variant peptides. Overall, TG40-H231, TG40-

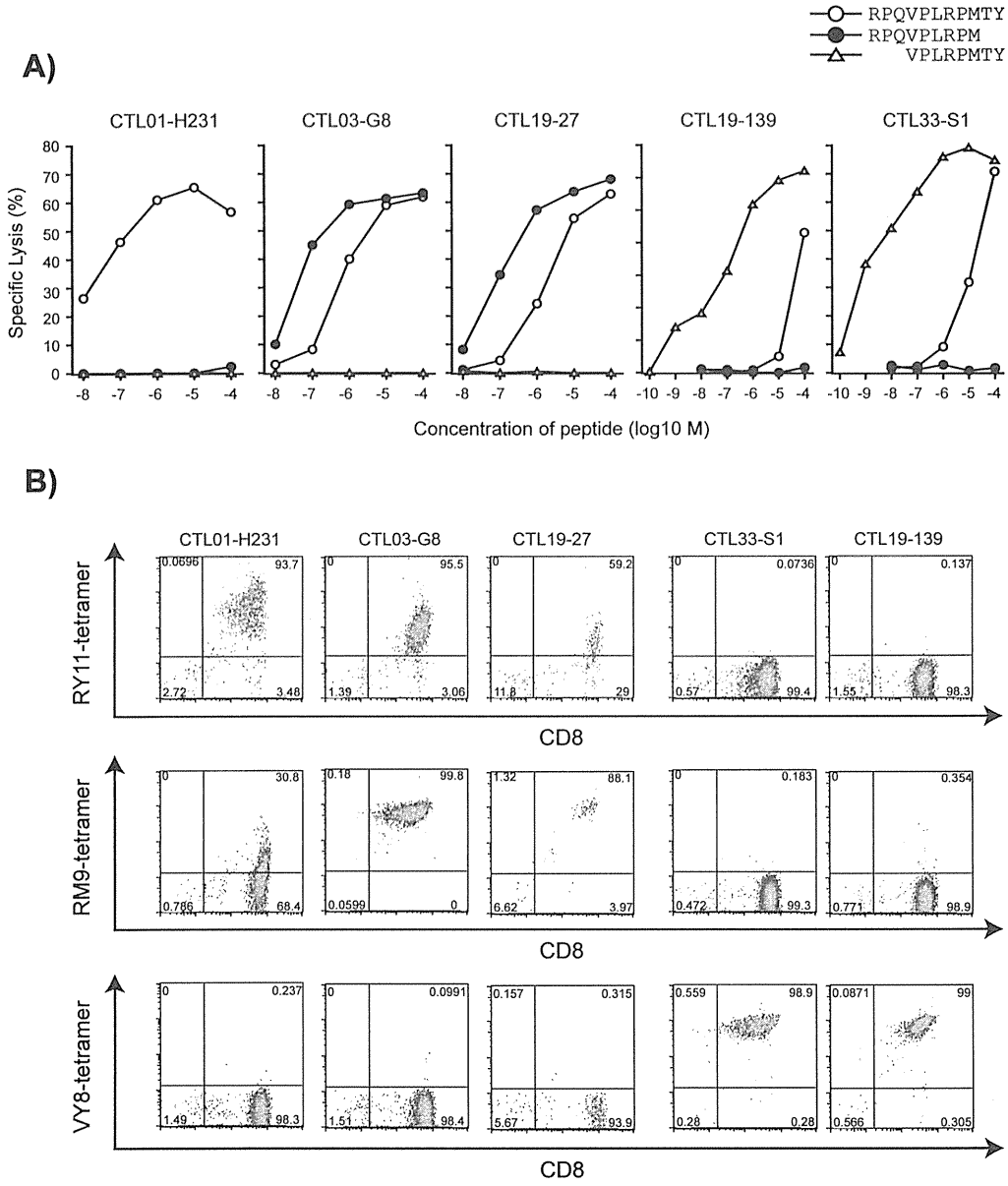

Fig. 2. Specificity of CTL clones toward overlapping epitopic peptides. A) Cytotoxic activity of CTL clones (CTL01-H231, CTL03-G8, CTL19-27, CTL19-139, and CTL33-S1) toward overlapping peptides is shown. As target cells, C1R cells expressing HLA-B*35:01 (C1R-B3501) were pulsed with various concentrations of RY11, RM9 or VY8 peptides. Data presented are the mean of duplicate assays. B) CTL clones were stained with HLA-B35 tetramers in complex with RY11, RM9 or VY8. Live $CD3^+$ cells were gated and analyzed for antigen specificity by binding with HLA-B35 tetramers.

G8, and TG40-27 retained reactivity towards 72, 45, and 46 out of the 198 variant peptides tested (36.4%, 22.7%, and 23.2% recognition, respectively; Fig. 4). Interestingly, although TG40-G8 and TG40-27 showed cross-reactivity towards only some amino acid variations at P1-P9, they showed cross-reactivity toward most amino acid residues at P10 and P11, suggesting that these peptides likely bound to HLA-B*35:01 with extending two amino acids at the C-terminus from the peptide-binding region, rather than their central region bulging for TCR-binding, as shown previously from crystal structural data [7,32]. This observation was consistent with the length preference of RM9 peptide by these TCRs, as was shown above. However, it is not clear why neither TG40-G8 nor -27 recognized Pro at P10 (Fig. 4). In contrast, TG40-H231 efficiently recognized all mutations at P8 of RY11, whereas these cells showed limited cross-recognition toward hydrophobic residues at P11 (Fig. 4). We also tested cross-reactivity profiles of TG40-139 and TG40-S1 by using 144 RY11-variant peptides containing mutations from P4 to P11, which corresponded to P1 to P8 of the VY8 sequence. TG40-139 and TG40-S1 showed unique cross-reactivity footprints compared with the other TCRs tested. All these data suggest that TCRs having similar peptide-length preference showed cross-recognition patterns related to the amino acid variations in the epitope peptides.

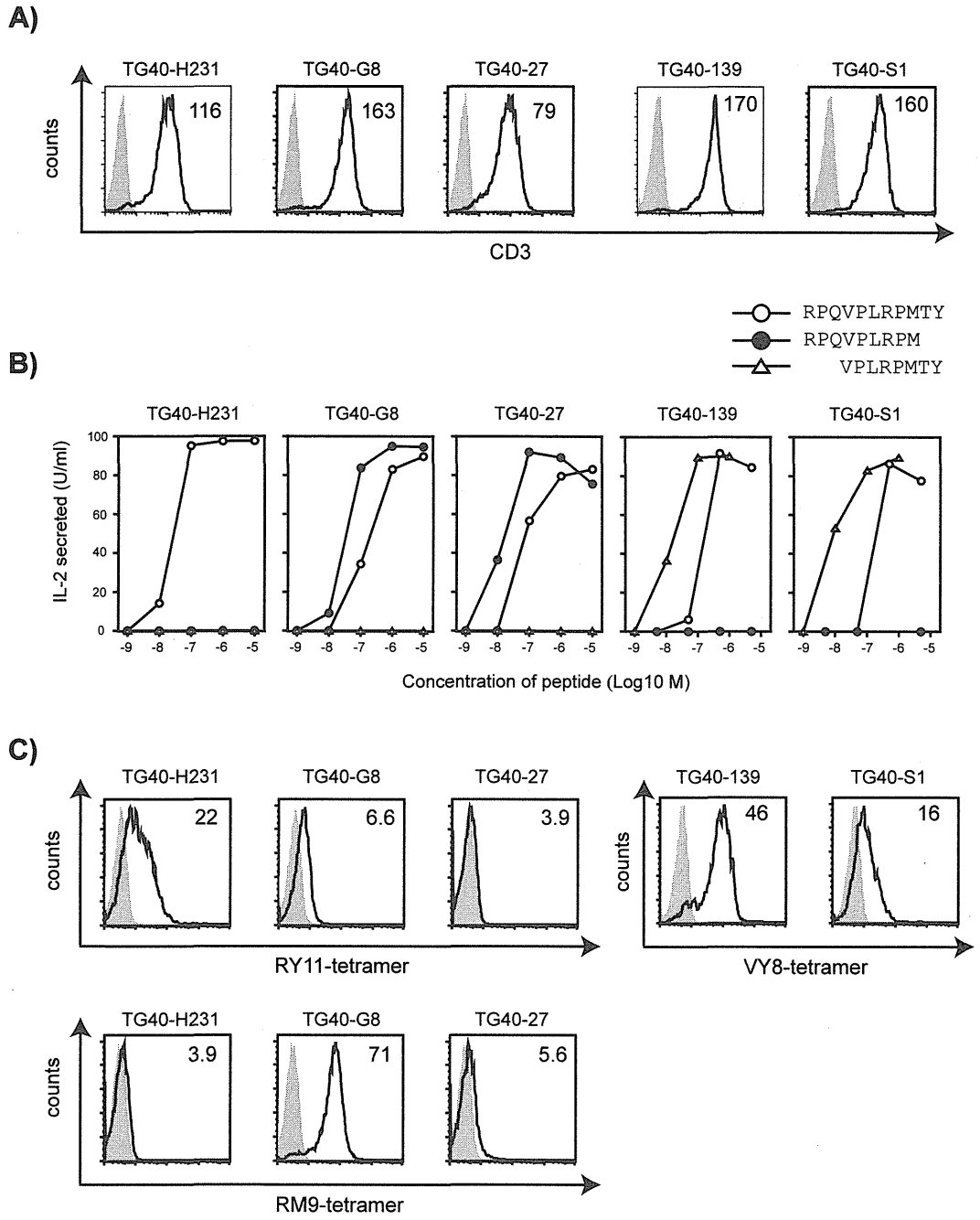

Fig. 3. Specificity analysis of reconstructed TCRs from H231, G8, 27, 139, and S1 CTL clones were reconstructed on TCR-deficient TG40 cells. A) Cell-surface expression of reconstructed TCRs was evaluated by staining with PE-conjugated anti-mouse CD3e mAb. The mean fluorescence intensity of CD3 expression is indicated in each histogram. The mock-transduced TG40 cells were used as a negative control (shaded). B) TG40/CD8 cells expressing the indicated TCRs were analyzed for their IL-2 secretion in response to various concentrations of the RY11, RM9 or VY8 peptides. The amount of IL-2 obtained for the mock-transduced TG40/CD8 was always <2.0. This assay was repeated three to four times for each peptide. C) HLA tetramer binding activity of TCR-transduced TG40 cells was analyzed. The mean fluorescence intensity of HLA tetramers is indicated in each histogram. The mock-transduced TG40 cells were used as a negative control (shaded), and the mean fluorescence intensity of these cells was <3.2.

4. Discussion

Here, we highlighted TCR fine specificity and cross-reactivity toward peptide-length variants as well as amino acid variations within the defined length of three HIV-1 Nef peptides by using a number of TCRs restricted by the same HLA-I molecule, HLA-B*35:01. Tetramer and peptide titration assays in combination with the TCR-reconstruction system revealed that the length preference of TCRs could be categorized into three types: mutually exclusive specificity toward RY11 or VY8 and cross-recognition toward RM9 and RY11. In addition, the cross-reactivity profiles toward amino acid variations of TCRs were unique and shared within the length-preference type but were very different between the

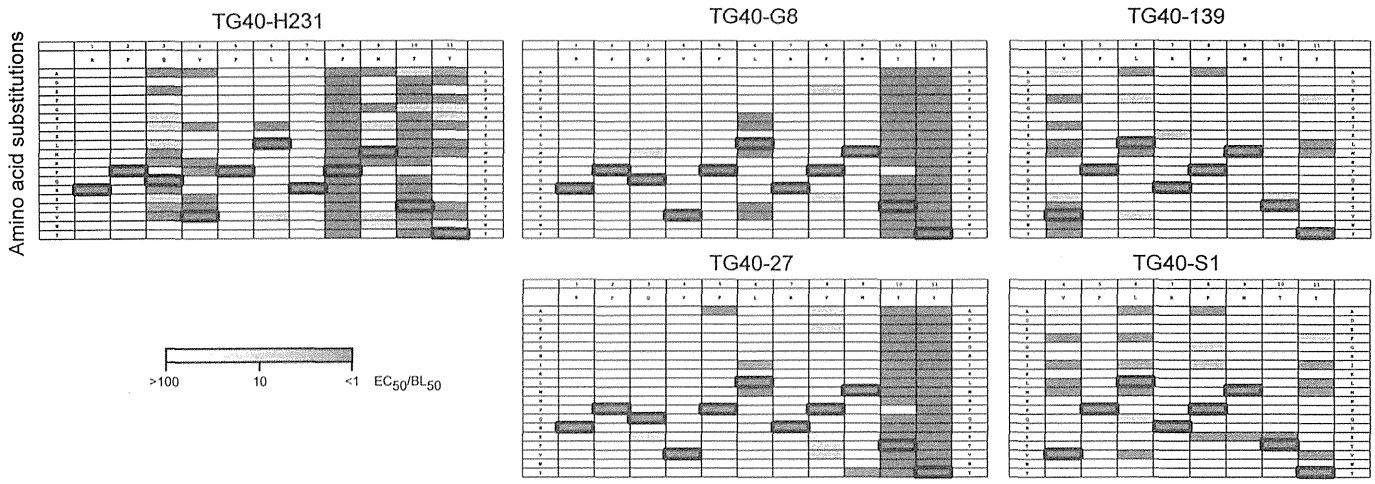

Fig. 4. Cross-reactivity footprints of TG40/CD8 cells expressing the indicated TCRs were tested for their capacity to recognize C1R-B3501 pulsed with each of 198 different peptides. The amino acid in each of the eleven positions in the RPQVPLRPMTY sequence was substituted by each of the 19 amino acids except for cysteine. The residues of the index peptide are listed horizontally at the top of the chart, and the letters along the sides indicate the residues replacing the index residue. The EC_{50} value of each peptide was calculated as the concentration of peptide that exhibited a half-maximal activation of TCR-transduced TG40 cells in response to 10^{-5} M index peptide defined as maximal. Amino acid substitution peptide analogs were tested for binding to HLA-B35 by using TAP-deficient RMA-S cells; and the concentration of the peptide that yielded a half maximal binding level (BL_{50}) was calculated as described earlier [22]. The TCR-pMHC interaction was determined by the EC_{50}/BL_{50} values, and >100 was defined as negative. The index residues at each position are outlined in black. This assay was repeated three to four times for each variant peptide.

three types. These results suggest that the length of the epitope peptide substantially influenced the cross-reactivity profiles of the cognate TCRs toward variant antigens.

The overlapping epitopes of different lengths presented by the same HLA-I are widely observed in HIV-1 infection: for example, HLA-B27-restricted Gag epitopes, KL8 (Gag263-270: KRWIILGL) and KK10 (Gag263-272: KRWIILGLNK) [7]; HLA-B57-restricted Gag peptides, KI8 (Gag162-169: KAFSPEVI) and KF11 (Gag162-172: KAFSPEVIPMF) [8]; HLA-B*54:01-restricted Pol epitopes, FT8 (Pol155-162: FPISPIET), FV9 (Pol155-163: FPISPIETV), FP10 (Pol155-164: FPISPIETVP), and FV11 (Pol 155-165: FPISPIETVPV) [9]. In all of these cases, each of these epitopes generated different CD8 T subsets; although only one of each overlapping epitopes can often be dominant *in vivo* [7–9]. In the HLA-B*35:01-restricted overlapping epitope case here, VY8 is a dominant epitope in the early phase of an HIV-1 infection, whereas RY11 becomes dominant in the chronic phase [21]; although the RM9-specific response *in vivo* has not been systematically analyzed yet. The pathways and mechanisms by which one of these epitopes becomes dominant over the others remain elusive. It would be interesting to determine the susceptibility of precursor peptides to proteasomes and other intracellular or ER-resident proteases such as ERAP1 [33] among these peptides in a future study. In contrast, it has been reported that the VY8/HLA-B35 complex shows more stability than the RY11/HLA-B35 complex in heat-denaturation experiments [6] and that such a difference in biochemical property between peptide-HLA complexes, rather than interaction between TCR and peptide-HLA complex is most likely associated with potent antiviral activity toward HIV-infected $CD4^+$ T lymphocytes by the VY8-specific CTLs [6,21]. It will therefore be intriguing to determine the thermostability profiles of all of these complexes between HLA-I molecule and overlapping peptides and compare their association with immunodominant hierarchy as well as with the antiviral potency of T lymphocytes recognizing these epitopes.

We previously found that the Arg to Thr and Tyr to Phe mutations at the position 1 and 11 in the RY11 sequence were associated with escape from CTL responses specific for RY11 and VY8, respectively [5]. Consistently, we showed here that RY11-specific TCRs (such as H231) failed to recognize peptides having the mutations at the position 1 and that VY8-specific TCRs (such as 139 and S1) were substantially reduced recognition toward the peptide with the mutation at the C-terminus (Fig. 4). These results suggest that the differential cross-reactivity profiles of TCRs specific for overlapping epitopes of different lengths contribute, at least in part, in forming sequence polymorphisms of naturally-arising CTL-escape viral variants at a population level.

One may raise a question how RM9-specific TCRs can recognize both RM9 and RY11 although RY11- and VY8-specific TCRs can only recognize the cognate peptides. In this regard, the crystal structure analyses of the peptide-HLA complexes show that the peptide can be bound with HLA in a C-terminally-extended way in some settings and that such complexes are recognized by the cognate TCRs [7,32]. It might be likely that a fraction of RY11 can be eventually bound with HLA-B*35:01 in a C-terminally-extended way and recognized by RM9-specific TCRs. Further structural study is needed to clarify whether a peptide can be bound with HLA with different modes: i.e., a C-terminal extended way or a central region bulged.

The TCR reconstruction system used here showed tetramer binding activity mostly consistent with the data generated by

CTL clones except in the case of TG40-27. This TCR-reconstructed cell showed extremely weak or virtually no binding activity toward RY11/B35 or RM9/B35 tetramers (Fig. 3C), although CTL19-27 bound to both tetramers (Fig. 2B). TCR-tetramer binding on the T cell surface may be influenced by several factors [34] such as TCR-peptide-HLA binding activity itself [35], expression level of TCRs on the cell surface [36], membrane architecture of T cells [37], co-receptors including CD8 [35,38], and so on. Given that TG40-27 responded to peptide-pulsed cells when human CD8 was expressed on the cell surface, it is likely that antigen recognition by the TCR from CTL19-27 was CD8 dependent, as previously described in the case of other TCR specificities [35,38]. Further experiments are needed to reveal the possible difference in antiviral activity of CTLs whose antigen recognition is dependent or independent on co-receptors.

Acknowledgments

This research was supported by a grant-in-aid for scientific research from the Ministry of Education, Science, Sports, and Culture (MEXT) of Japan; by the Global COE Program (Global Education and Research Center Aiming at the Control of AIDS), MEXT, Japan; and by a grant-in-aid for AIDS research from the Ministry of Health, Labor, and Welfare of Japan.

References

[1] Rudolph MG, Stanfield RL, Wilson IA. How TCRs bind MHCs, peptides, and coreceptors. Annu Rev Immunol 2006;24:419–66.
[2] Tynan FE, Burrows SR, Buckle AM, Clements CS, Borg NA, Miles JJ, et al. T cell receptor recognition of a 'super-bulged' major histocompatibility complex class I-bound peptide. Nat Immunol 2005;6:1114–22.
[3] Ekeruche-Makinde J, Miles JJ, van den Berg HA, Skowera A, Cole DK, Dolton G, et al. Peptide length determines the outcome of TCR/peptide-MHCI engagement. Blood 2013;121:1112–23.
[4] Burrows JM, Bell MJ, Brennan R, Miles JJ, Khanna R, Burrows SR. Preferential binding of unusually long peptides to MHC class I and its influence on the selection of target peptides for T cell recognition. Mol Immunol 2008;45:1818–24.
[5] Ueno T, Motozono C, Dohki S, Mwimanzi P, Rauch S, Fackler OT, et al. CTL-mediated selective pressure influences dynamic evolution and pathogenic functions of HIV-1 Nef. J Immunol 2008;180:1107–16.
[6] Motozono C, Yanaka S, Tsumoto K, Takiguchi M, Ueno T. Impact of intrinsic cooperative thermodynamics of peptide-MHC complexes on antiviral activity of HIV-specific CTL. J Immunol 2009;182:5528–36.
[7] Tenzer S, Wee E, Burgevin A, Stewart-Jones G, Friis L, Lamberth K, et al. Antigen processing influences HIV-specific cytotoxic T lymphocyte immunodominance. Nat Immunol 2009;10:636–46.
[8] Goulder PJ, Tang Y, Pelton SI, Walker BD. HLA-B57-restricted cytotoxic T-lymphocyte activity in a single infected subject toward two optimal epitopes, one of which is entirely contained within the other. J Virol 2000;74:5291–9.
[9] Hashimoto M, Akahoshi T, Murakoshi H, Ishizuka N, Oka S, Takiguchi M. CTL recognition of HIV-1-infected cells via cross-recognition of multiple overlapping peptides from a single 11-mer Pol sequence. Eur J Immunol 2012;42:2621–31.
[10] Lucchiari-Hartz M, Lindo V, Hitziger N, Gaedicke S, Saveanu L, van Endert PM, et al. Differential proteasomal processing of hydrophobic and hydrophilic protein regions: contribution to cytotoxic T lymphocyte epitope clustering in HIV-1-Nef. Proc Natl Acad Sci U S A 2003;100:7755–60.
[11] Rehermann B, Chisari FV. Cell mediated immune response to the hepatitis C virus. Curr Top Microbiol Immunol 2000;242:299–325.
[12] Dong T, Stewart-Jones G, Chen N, Easterbrook P, Xu X, Papagno L, et al. HIV-specific cytotoxic T cells from long-term survivors select a unique T cell receptor. J Exp Med 2004;200:1547–57.
[13] Kosmrlj A, Read EL, Qi Y, Allen TM, Altfeld M, Deeks SG, et al. Effects of thymic selection of the T-cell repertoire on HLA class I-associated control of HIV infection. Nature 2010;465:350–4.
[14] Iglesias MC, Almeida JR, Fastenackels S, van Bockel DJ, Hashimoto M, Venturi V, et al. Escape from highly effective public CD8+ T-cell clonotypes by HIV. Blood 2011;118:2138–49.
[15] Chen H, Ndhlovu ZM, Liu D, Porter LC, Fang JW, Darko S, et al. TCR clonotypes modulate the protective effect of HLA class I molecules in HIV-1 infection. Nat Immunol 2012;13:691–700.
[16] Hoof I, Perez CL, Buggert M, Gustafsson RK, Nielsen M, Lund O, et al. Interdisciplinary analysis of HIV-specific CD8+ T cell responses against variant epitopes reveals restricted TCR promiscuity. J Immunol 2010;184:5383–91.
[17] Ladell K, Hashimoto M, Iglesias MC, Wilmann PG, McLaren JE, Gras S, et al. A, Molecular basis for the control of preimmune escape variants by HIV-specific CD8(+) T cells. Immunity 2013;38:425–36.
[18] Culmann-Penciolelli B, Lamhamedi-Cherradi S, Couillin I, Guegan N, Levy JP, Guillet JG, et al. Identification of multirestricted immunodominant regions recognized by cytolytic T lymphocytes in the human immunodeficiency virus type 1 Nef protein. J Virol 1994;68:7336–43.
[19] Choppin J, Cohen W, Bianco A, Briand JP, Connan F, Dalod M, et al. Characteristics of HIV-1 Nef regions containing multiple CD8+ T cell epitopes: wealth of HLA-binding motifs and sensitivity to proteasome degradation. J Immunol 2001;166:6164–9.
[20] Milicic A, Price DA, Zimbwa P, Booth BL, Brown HL, Easterbrook PJ, et al. CD8+ T cell epitope-flanking mutations disrupt proteasomal processing of HIV-1 Nef. J Immunol 2005;175:4618–26.
[21] Ueno T, Idegami Y, Motozono C, Oka S, Takiguchi M. Altering effects of antigenic variations in HIV-1 on antiviral effectiveness of HIV-specific CTLs. J Immunol 2007;178:5513–23.
[22] Ueno T, Tomiyama H, Takiguchi M. Single T cell receptor-mediated recognition of an identical HIV-derived peptide presented by multiple HLA class I molecules. J Immunol 2002;169:4961–9.
[23] Ueno T, Tomiyama H, Fujiwara M, Oka S, Takiguchi M. HLA class I-restricted recognition of an HIV-derived epitope peptide by a human T cell receptor alpha chain having a Vdelta1 variable segment. Eur J Immunol 2003;33:2910–6.
[24] Smith KJ, Reid SW, Stuart DI, McMichael AJ, Jones EY, Bell JI. An altered position of the alpha 2 helix of MHC class I is revealed by the crystal structure of HLA-B*3501. Immunity 1996;4:203–13.
[25] Gerber PR, Muller K. MAB, a generally applicable molecular force field for structure modelling in medicinal chemistry. J Comput Aided Mol Des 1995;9:251–68.
[26] Onufriev A, Bashford D, Case DA. Modification of the generalized born model suitable for macromolecules. J Phys Chem B 2000;104:3712–20.
[27] Goto J, Kataoka R, Muta H, Hirayama N. ASEDock-docking based on alpha spheres and excluded volumes. J Chem Inf Model 2008;48:583–90.
[28] Tomiyama H, Miwa K, Shiga H, Moore YI, Oka S, Iwamoto A, et al. Evidence of presentation of multiple HIV-1 cytotoxic T lymphocyte epitopes by HLA-B*3501 molecules that are associated with the accelerated progression of AIDS. J Immunol 1997;158:5026–34.
[29] Rowland-Jones S, Sutton J, Ariyoshi K, Dong T, Gotch F, McAdam S, et al. HIV-specific cytotoxic T-cells in HIV-exposed but uninfected Gambian women. Nat Med 1995;1:59–64.
[30] Rist MJ, Theodossis A, Croft NP, Neller MA, Welland A, Chen Z, et al. HLA peptide length preferences control CD8+ T cell responses. J Immunol 2013;191:561–71.
[31] Hornell TM, Martin SM, Myers NB, Connolly JM. Peptide length variants p2Ca and QL9 present distinct conformations to L(d)-specific T cells. J Immunol 2001;167:4207–14.
[32] Collins EJ, Garboczi DN, Wiley DC. Three-dimensional structure of a peptide extending from one end of a class I MHC binding site. Nature 1994;371:626–9.

[33] York IA, Chang SC, Saric T, Keys JA, Favreau JM, Goldberg AL, et al. The ER aminopeptidase ERAP1 enhances or limits antigen presentation by trimming epitopes to 8-9 residues. Nat Immunol 2002;3:1177–84.
[34] Wooldridge L, Lissina A, Cole DK, van den Berg HA, Price DA, Sewell AK. Tricks with tetramers: how to get the most from multimeric peptide-MHC. Immunology 2009;126:147–64.
[35] Laugel B, van den Berg HA, Gostick E, Cole DK, Wooldridge L, Boulter J, et al. Different T cell receptor affinity thresholds and CD8 coreceptor dependence govern cytotoxic T lymphocyte activation and tetramer binding properties. J Biol Chem 2007;282:23799–810.
[36] Lissina A, Ladell K, Skowera A, Clement M, Edwards E, Seggewiss R, et al. Protein kinase inhibitors substantially improve the physical detection of T-cells with peptide-MHC tetramers. J Immunol Methods 2009;340:11–24.
[37] Drake 3rd DR, Braciale TJ. Cutting edge: lipid raft integrity affects the efficiency of MHC class I tetramer binding and cell surface TCR arrangement on CD8+ T cells. J Immunol 2001;166:7009–13.
[38] Cole DK, Laugel B, Clement M, Price DA, Wooldridge L, Sewell AK. The molecular determinants of CD8 co-receptor function. Immunology 2012;137:139–48.

RETROVIROLOGY

RESEARCH Open Access

The phosphorylation of HIV-1 Gag by atypical protein kinase C facilitates viral infectivity by promoting Vpr incorporation into virions

Ayumi Kudoh[1], Shoukichi Takahama[2], Tatsuya Sawasaki[2,3], Hirotaka Ode[4,5], Masaru Yokoyama[5], Akiko Okayama[6], Akiyo Ishikawa[6], Kei Miyakawa[1], Satoko Matsunaga[1], Hirokazu Kimura[7], Wataru Sugiura[4], Hironori Sato[5], Hisashi Hirano[6], Shigeo Ohno[8], Naoki Yamamoto[9] and Akihide Ryo[1*]

Abstract

Background: Human immunodeficiency virus type 1 (HIV-1) Gag is the main structural protein that mediates the assembly and release of virus-like particles (VLPs) from an infected cell membrane. The Gag C-terminal p6 domain contains short sequence motifs that facilitate virus release from the plasma membrane and mediate incorporation of the viral Vpr protein. Gag p6 has also been found to be phosphorylated during HIV-1 infection and this event may affect virus replication. However, the kinase that directs the phosphorylation of Gag p6 toward virus replication remains to be identified. In our present study, we identified this kinase using a proteomic approach and further delineate its role in HIV-1 replication.

Results: A proteomic approach was designed to systematically identify human protein kinases that potently interact with HIV-1 Gag and successfully identified 22 candidates. Among this panel, atypical protein kinase C (aPKC) was found to phosphorylate HIV-1 Gag p6. Subsequent LC-MS/MS and immunoblotting analysis with a phospho-specific antibody confirmed both in vitro and in vivo that aPKC phosphorylates HIV-1 Gag at Ser487. Computer-assisted structural modeling and a subsequent cell-based assay revealed that this phosphorylation event is necessary for the interaction between Gag and Vpr and results in the incorporation of Vpr into virions. Moreover, the inhibition of aPKC activity reduced the Vpr levels in virions and impaired HIV-1 infectivity of human primary macrophages.

Conclusion: Our current results indicate for the first time that HIV-1 Gag phosphorylation on Ser487 is mediated by aPKC and that this kinase may regulate the incorporation of Vpr into HIV-1 virions and thereby supports virus infectivity. Furthermore, aPKC inhibition efficiently suppresses HIV-1 infectivity in macrophages. aPKC may therefore be an intriguing therapeutic target for HIV-1 infection.

Keywords: HIV-1 infection, Phosphorylation, Vpr, aPKC

Background

Human immunodeficiency virus type 1 (HIV-1), a causative agent of AIDS, is an intracellular parasite that has evolved to invade complex human systems and utilize its host machinery for its proliferation. A dynamic interplay between HIV-1 and its human host systems plays a crucial role in promoting virus replication. The identification of the host factors required for viral infection can provide further insights into the nature of HIV-1 replication pathways and assist with identifying new targets for anti-viral therapies. Recent studies have revealed that host factors are involved in the post-translational modification of viral proteins, such as phosphorylation and ubiquitination, thereby regulating HIV-1 replication and pathogenicity [1-3].

The *gag* gene of HIV-1 encodes both structural and functional proteins essential for the assembly and release of enveloped virus-like particles [4]. In the infected cell, Gag is synthesized as a 55-kDa polyprotein and assembled into spherical immature particles at plasma membrane.

* Correspondence: aryo@yokohama-cu.ac.jp
[1]Department of Microbiology, Yokohama City University School of Medicine, Yokohama, Kanagawa, Japan
Full list of author information is available at the end of the article

Concomitant with, or after these viral particles pinch off and are released from the host cell via budding, the virus-encoded protease becomes activated and cleaves Gag into its functional subdomains, matrix (MA, p17), capsid (CA, p24), and nucleocapsid (NC, p7), as well as several shorter segments: SP1 (spacer peptide 1), SP2, and p6. This proteolytic maturation in tandem with the incorporation of viral enzymes and accessory proteins into virions results in the acquisition of HIV-1 infectivity [5-8].

Retroviral assembly can be subdivided into distinct stages of Gag membrane targeting, virus bud formation and induction of membrane curvature, and release of the newly assembled virus bud through a membrane fission event. HIV-1 budding from the cell surface depends on viral late domains within Gag p6 [9]. Two late domains have been identified within p6, the PTAP and $LYPX_nL$ motifs. The PTAP motif binds the cellular protein Tsg101 [10,11], whereas the $LYPX_nL$ motif is the docking site for Alix/AIP-1 [12,13]. Tsg101 functions in HIV-1 budding as a member of the Endosomal Sorting Complex Required for Transport-1 (ESCRT-I), which initiates the sorting of surface proteins into late endosomal compartments known as multivesicular bodies (MVB) [14,15]. Alix, ALG-2 interacting protein, functions in endosomal metabolism, promotes viral budding by interconnecting HIV-1 Gag with the ESCRT-III CHMP4 proteins [16,17].

Another important domain within Gag p6 is the C-terminal LXXLF domain. Interestingly, both the Leu486 and Leu491 residues in this motif are highly conserved and together with the downstream Phe492, comprise the LXXLF binding domain for the HIV-1 accessory viral protein R (Vpr) [18,19]. The substitution of residues in this domain causes a decrease in the Vpr incorporation levels compared with full-length HIV-1 Gag protein, indicating that this conserved region is essential for this process.

HIV-1 Vpr is a non-structural protein that is incorporated into the viral particles and possesses several characteristic features that are known to play important roles in HIV-1 replication and disease progression. Vpr mediates multiple functions, including the nuclear import of the HIV-1 pre-integration complex, G2 cell cycle arrest, the transactivation of both viral replication and host genes, and the induction of apoptosis [20]. Vpr interacts with the LXXLF binding domain of Gag p6 and is thereby packaged into the virus particles. Virion-incorporated Vpr is known to positively regulate the infection of non-dividing cells and enhance virus production in macrophages and in resting T cells. However, it remains elusive whether and how Vpr incorporation is indeed regulated. Furthermore, although p6 has been shown to be post-translationally modified by phosphorylation [2,21,22], it is unknown whether this phosphorylation event has any functional relevance to Vpr incorporation and HIV-1 infectivity.

In our current study, we utilized an in vitro high-throughput protein-protein interaction assay using full-length HIV-1 Gag and host protein kinases synthesized by the wheat germ cell-free protein production system in an attempt to identify the kinase (s) that directs the phosphorylation of Gag p6 to promote virus replication. We here report that atypical protein kinase C (aPKC) is a functional interactor of HIV-1 Gag and facilitates viral infectivity by promoting the incorporation of Vpr into virions. We provide evidence that Gag Ser487 (p6 Ser40) is phosphorylated by aPKC, and that this phosphorylation is essential for p6-Vpr interactions and the resultant Vpr incorporation within viral particles. Using computer-assisted structural modeling, we further explore the biological significance of the phosphorylation of Gag-p6 Ser487 by aPKC for the physiological interaction between Gag and Vpr. Our current study sheds new light on the molecular link between Gag phosphorylation and viral infectivity through the incorporation of Vpr into virions.

Results

aPKC binds and phosphorylates HIV-1 Gag

Our initial goal was to identify host kinases that phosphorylate the HIV-1 Gag protein. Because Gag phosphorylation is important for its functional role, we focused on human protein kinases as potential Gag regulators. We synthesized more than 287 full-length protein kinases using a wheat germ cell-free protein production system, and screened them for their association with Gag with the amplified luminescent proximity homogenous assay (AlphaScreen) [23]. In this method, the extent of the protein-protein interaction was measured by assaying the luminescence intensity (Figure 1A). Full-length Gag and human protein kinases were synthesized using a wheat germ cell-free system and subjected to an AlphaScreen assessment. The binding efficiency of HIV-1 Gag with each kinase was normalized relative to the luminescent activity of a control DHFR protein (Figure 1B). When a relative light unit per cutoff (RLU/Co) ratio of ≥ 3.0 was used as the threshold, we found that 22 host kinases could selectively interact with HIV-1 Gag and thus were identified as primary kinase candidates for the phosphorylation of HIV-1 Gag (Figure 1B).

Our assay detected Erk2 and PKCβ as Gag interactors (S/N = 1.76 and 1.17, respectively), both of which have been already reported to phosphorylate Gag during HIV-1 infection [2,22,24,25]. This validated our screening approach. Interestingly, we further found that the aPKC family kinases, PKCζ and PKCι, could interact with HIV-1 Gag at a relatively high score (S/N = 3.57 and 3.19, respectively). PKCζ and PKCι share a more than 70% amino acid identity in entire protein sequence and 84% in the catalytic domain, and an almost identical

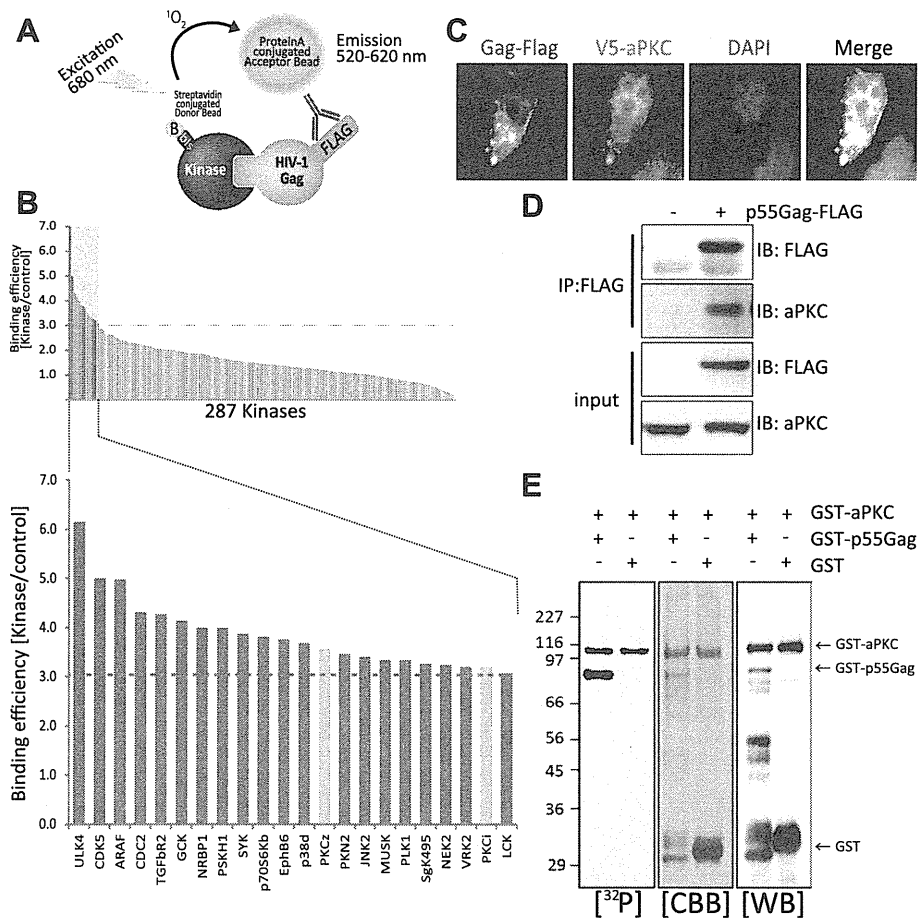

Figure 1 aPKC phosphorylates HIV-1 Gag. (A) Schematic representation of the AlphaScreen based luminescent system used to screen for human kinases that interact with HIV-1 Gag. Briefly, HIV-1 Gag was incubated with each human protein kinase and protein A-conjugated acceptor beads with anti-FLAG antibody and streptavidin coated donor beads were added and bound to the tagged substrate. Upon laser excitation, the donor beads convert ambient oxygen to singlet oxygen. When a molecular interaction occurs between HIV-1 Gag and a particular kinase, singlet oxygen transfers across to activate the acceptor beads and subsequently emit light at 520–620 nm. **(B)** HIV-1 Gag interacting kinases identified from a human kinase protein library. **(C)** Confocal microscopy analysis of V5-aPKC (Alexa 568) and Gag-Flag (Alexa 488) in 293T cells. **(D)** Immunoprecipitation of Gag with aPKC. 293T cells were transfected with Flag tagged Gag and cell lysates were immunoprecipitated with anti-Flag antibody 48 hours later. Samples were then probed with anti-aPKC and anti-Flag antibodies. Bottom panel shows input for pull-down assay. **(E)** *In vitro* phosphorylation of HIV-1 Gag by aPKC. GST, GST tagged aPKC and Gag proteins were expressed and affinity-purified from wheat germ cell-free extract. aPKC-mediated phosphorylation was assessed by incubating recombinant GST or GST-Gag with recombinant active GST-aPKC in the presence of [γ-^{32}P] ATP. The reaction products were analyzed by autoradiography, Coomassie Brilliant Blue (CBB) stain and blotted with GST antibody.

substrate specificity [26]. We thus focused on aPKC as a previously uncharacterized Gag-interacting factor for further in depth functional analysis.

To better understand the functional relevance of aPKC in HIV-1 infection, we first examined the subcellular localization of both HIV-1 Gag protein and aPKC protein in 293T cells by immunofluorescent analysis. 293T cells were transfected with Flag tagged HIV-1 Gag and V5-aPKC expression vector. Gag-Flag displayed a punctate expression pattern in the cytoplasm and a partial co-localization with aPKC in cytoplasm and plasma membrane (Figure 1C).

We performed immunoprecipitation analysis and found that aPKC could bind Gag in cells (Figure 1D). We next examined whether aPKC can directly phosphorylate HIV-1 Gag protein in vitro. Recombinant GST-Gag or GST proteins were expressed and purified from wheat germ cell-free extract by glutathione sepharose beads and used as substrates for in vitro kinase assays. aPKC was found to phosphorylate GST-Gag but not GST, with a prominent auto-phosphorylation of aPKC also observed (Figure 1E). These data together indicate that aPKC binds and phosphorylates HIV-1 Gag.

aPKC phosphorylates the Ser487 residue of HIV-1 Gag

We next sought to determine the sites of aPKC phosphorylation in HIV-1 Gag. GST-Gag was incubated with recombinant aPKC for their phosphorylation and this

mixture was then processed for proteomic analysis. Initial phosphorylation site analysis was performed using the data dependent of tandem matrix-assisted laser desorption Ionization-time of flight mass spectrometry (MALDI-TOF/TOF-MS), followed by in depth analysis with selected peptides through data collection. Fragmentation of this peptide by MS/MS produced a spectrum through which we identified one of the b-ions and 10 of the y-ions matching the sequence QEPIDKELYPLTpSLR. Tandem mass spectra of the signals at m/z 1881.95, m/z 1783.95(neutral loss) and m/z 1801.97 revealed sequences corresponding to the unmodified, mono- phospho peptide of Gag-p6 (QEPIDKELYPLTpSLR; Figure 2). Furthermore, a Mascot search result identified the sequence QEPIDKELYPLTpSLR (score 73). The Ser487 site was found to be located at Ser40 of Gag-p6 domain in close proximity to both $LYPX_nL$ and LXXLF motif.

Based on our MS analysis, we constructed a GST-tagged p6 and its site-directed mutant GST-p6-Ser487Ala (S487A) and GST-p6-Ser461Ala (S461A) as a negative control. Subsequent in vitro kinase assay results demonstrated that GST-p6 is phosphorylated by aPKC, but not GST-p6-S487A (Figure 3A). These results suggested that aPKC indeed phosphorylates the Ser487 residue of HIV-1 Gag *in vitro*.

To further assess the phosphorylation of Gag at Ser487, we generated a polyclonal antibody against phosphoryated-Ser487 (pS487). We initially confirmed the specificity and sensitivity of the antibody using the AlphaScreen system. We found that our antibody recognized only Ser487 phosphorylated peptides but neither a non-phosphorylated peptide nor a peptide harboring a Ser487 to Ala substitution (Figure 3B). We then used this antibody for in depth cell culture study. 293T cells were transfected with V5 tagged wild type aPKC or a kinase-negative mutant (aPKC-Kn), together with wild type Gag-Pol. A marked increase in the level of Gag phosphorylation at Ser487 was observed in cells expressing the wild type aPKC, whereas there was no obvious increase in the amounts of phosphorylation in either aPKC-Kn or mock transfected cells (Figure 3C). These observations clearly indicate that the expression of aPKC leads to the phosphorylation of HIV-1 Gag at Ser487 in cells, and that this phosphorylation is dependent of the kinase activity of aPKC.

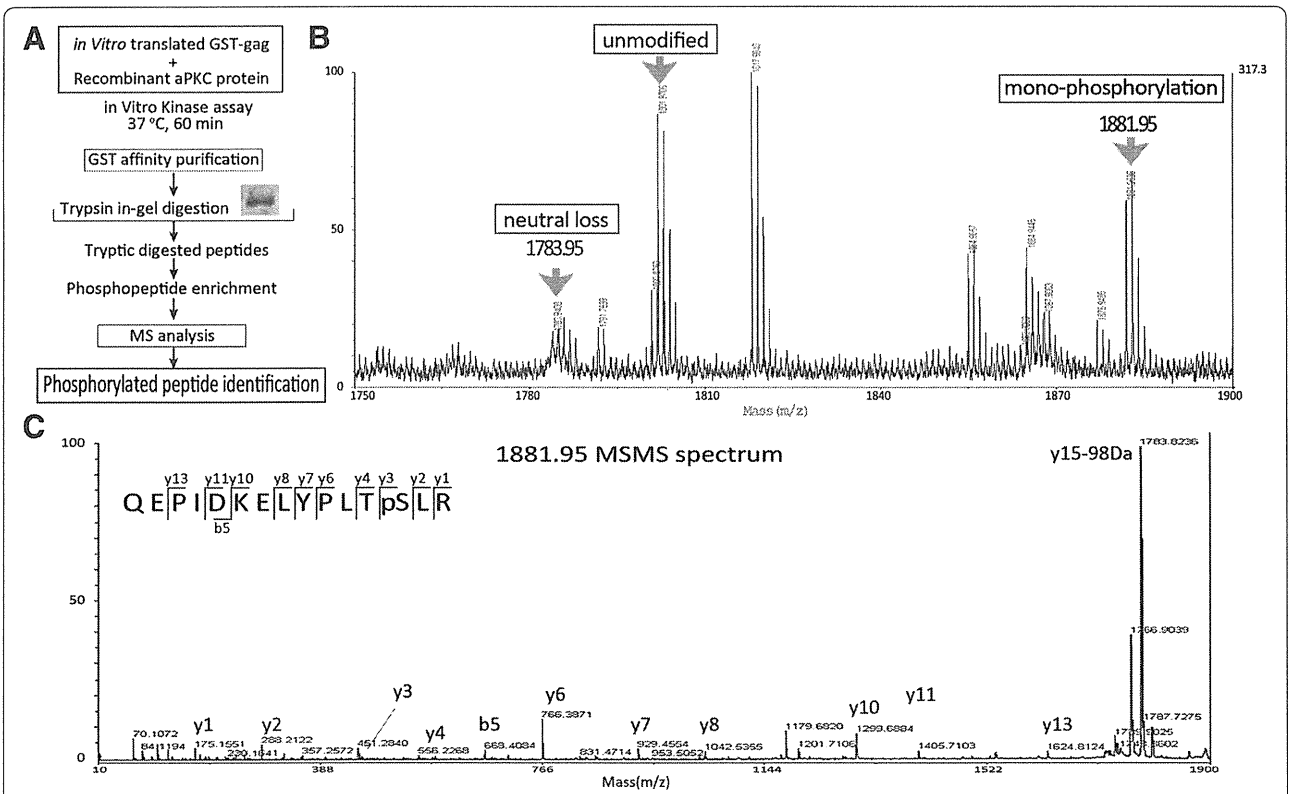

Figure 2 Identification of the phosphorylated Gag-p6 site. (A) Schematic overview of the experimental workflow. **(B)** MS peptide map of phosphorylated GST-Gag after trypsin digestion. The red arrow indicates the 1881.95 Da peak which is unique to the sample treated with active aPKC. This is consistent with the mass of the theoretical phosphorylated peptides and the map shows a neutral loss peak at 1783.95. **(C)** The resulting phosphopeptide was analyzed using MALDI-TOF/TOF MS. Fragment ions of the b and y-series identified in the tandem mass spectra from the peptide are shown. Tandem mass spectra of m/z 1881.95 signals revealed that each sequence corresponded to the phosphopeptide (QEPIDKELYPLTpSLR) of Gag-P6.

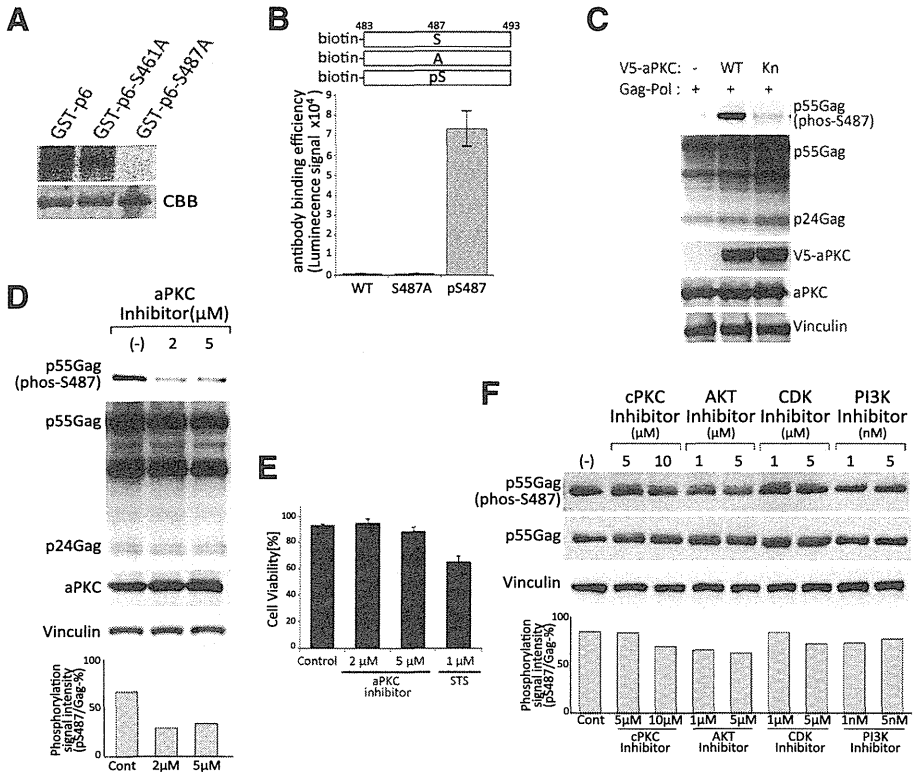

Figure 3 aPKC phosphorylates HIV-1 Gag on Ser487. (A) GST-p6, GST-p6S461A or GST-p6S487A proteins were expressed and affinity-purified from wheat germ cell-free extracts. aPKC-mediated phosphorylation was assessed by incubating recombinant GST-p6, GST-p6S461A or GST-p6S487A with recombinant active GST-aPKC in the presence of [γ-^{32}P] ATP for 60 min at 37°C. The reaction products were analyzed by autoradiography and Coomassie Brilliant Blue (CBB) staining. **(B)** Assessment of phospho-Ser487 antibody specificity and binding efficiency using the AlphaScreen system. Biotin tagged peptides were incubated with phospho-Ser487 specific antibodies for. The graph shows the luminescence signal intensity which represents antibody binding efficiency. Each value is the mean of three independent experiments. **(C)** 293T cells were transfected with wild type Gag-pol and either V5 tagged wild type aPKC (WT) or kinase-negative aPKC (Kn). Whole-cell extracts were prepared, and equal amounts of proteins for each sample were separated by SDS-PAGE and subjected to western blot analysis using indicated antibodies. **(D)** Effects of aPKC inhibitor on the phosphorylation of Gag-Ser487. 293T cells were transfected with Gag-pol expression vector and cultured in the presence of the indicated concentrations of aPKC inhibitor. Clarified cell lysates were prepared and equal amounts of proteins were subjected to SDS-PAGE, followed by western blot analysis using indicated antibodies. Densitometry analysis of the p55Gag (pS487)/p55Gag bands in the western blot is shown in the bottom panel. **(E)** Effects of aPKC inhibitor on viability of 293T cells. 293T cells were treated with aPKC inhibitor (2 or 5 μM) or 1 μM Staurosporine (STS) and analysed for cell viability using trypan blue exclusion at 48 hours. **(F)** Effects of kinase specific inhibitors on the phosphorylation of Gag-Ser487. 293T cells were transfected with Gag-pol expression vector and treated with inhibitors against cPKC, AKT, CDK and PI3K. Cell lysates were prepared and analyzed as described in **(D)**.

To further investigate whether the phosphorylation of HIV-1 Gag at Ser487 is mediated by endogenous aPKC activity, we employed a myristoylated PKCζ pseudosubstrate peptide as an aPKC inhibitor. This PKCζ pseudosubstrate peptide mimics the substrate binding site in PKCζ (113–125) and PKCι (114–126), and suppresses the activity of endogenous PKCι and PKCζ. HIV-1 Gag-Pol expression plasmids were transfected into 293T cells with or without aPKC inhibitor treatment. Immunoblot analysis revealed that the aPKC inhibitor suppressed Gag phosphorylation at Ser487. Subsequent titration analysis demonstrated a dose-dependent inhibitory effect of the PKCζ pseudosubstrate peptide by showing an 74.9% and 70.4% decrease in Gag phosphorylation at 2 μM and 5 μM doses, respectively (Figure 3D). Note that at these concentrations the aPKC inhibitor did not affect the expression levels of endogenous aPKC as well as a house-keeping protein Vinculin (Figure 3D). Furthermore, cell viability was not prominently affected by aPKC inhibitor when cells were assessed by trypan blue exclusion (Figure 3E). Conventional PKC (PKCα, PKCβ), Akt, CDK and PI3 kinases have been reported previously to affect HIV-1 replication through their phosphorylation of HIV-1 or of host proteins [3,24,27-30]. We thus also investigated using specific inhibitors whether these kinases could mediate the phosphorylation of HIV-1 Gag at Ser487. Our results show that neither PKCα nor PKCβ specific pseudosubstrates affect Gag phosphorylation at Ser487 (Figure 3F). Similarly, neither Akt inhibitor, the CDK inhibitor roscovitine nor the PI3K inhibitor wortmannin blocked Gag phosphorylation at Ser487 (Figure 3F). Taken together, these observations

indicate that aPKC specifically phosphorylates HIV-1 Gag at Ser487 both *in vitro* and *in vivo*.

The phosphorylation of Gag Ser487 facilitates the interaction between Gag and Vpr

HIV-1 Gag p6 contains a late domain consisting of three protein binding motifs, PTAP (Tsg101 binding), LYPXnL (Alix binding) and C-terminal Vpr. Ser487 is located in the Alix binding motif and is also adjacent to the Vpr binding motif spanning amino acids 488–492 (Figure 4A). To obtain structural-based information on Gag phosphorylation on Ser487 and how it affects the interaction of Gag with Alix or Vpr, we conducted computer-assisted molecular modeling of the Gag p6 domain coupled with peptides derived from either Alix or Vpr. The models constructed in this study included unphosphorylated and phosphorylated Gag-p6 (amino acids Tyr483-Ser494), and its Ser/Ala substituted mutant on Ser487 (S487A). Molecular modeling calculations with thermodynamically optimized three dimensional structures showed less than 1 Å of positional shifts of Cα atoms of Gag-p6 by phosphorylation, suggesting no obvious difference in the basic structure of Gag-p6 irrespective of the phosphorylation status. Furthermore, binding interface between Gag-p6 and Alix was not affected by the phosphorylation (Figure 4B, Upper panels) or Ser/Ala substitution of Gag Ser487 [31-33]. On the other hands, the binding of Gag-p6 with Vpr was facilitated since the phosphorylation of Ser487 can create another hydrogen bond between Gag-p6 and Vpr (Figure 4B, Lower panels). The Ser487 was predicted to form no hydrogen bonds with Vpr in non-phosphorylated state, whereas the phosphorylated Ser487 could form the hydrogen bond with Gln44 of Vpr. Consequently, binding energy calculated with Molecular Operating Environment (MOE) was significantly increased by phosphorylation of Ser487 only for the Gag-p6-Vpr complex (Figure 4B, tables). These data suggest that the phosphorylation of Gag-p6 on Ser487 could indeed affect the binding affinity of Gag-p6 with Vpr but not Alix.

Based on our structural modeling results, we next asked whether the phosphorylation of Gag at Ser487 has

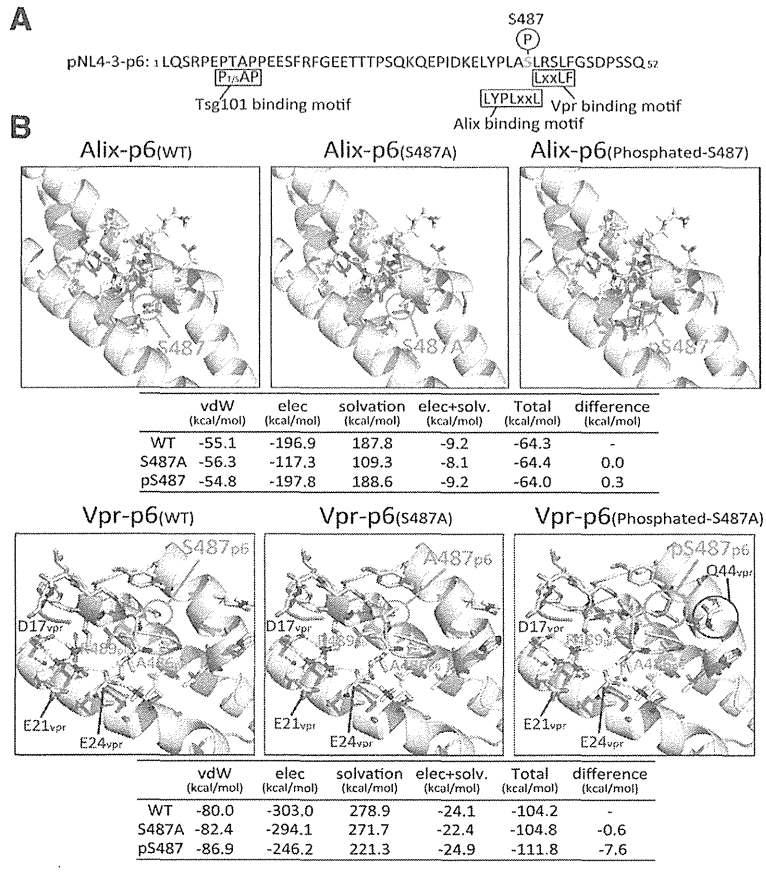

Figure 4 The phosphorylation of Gag at Ser487 facilitates the interaction of Vpr and Gag-p6. (A) Schematic representation of the HIV-1 Gag-p6 sequence indicating the binding motifs, Tsg101, Alix and Vpr, located around the Ser487 site. **(B)** Complex structure models of Gag-p6 with Alix or Vpr. The structural calculations were undertaken using MOE. Upper panel shows structural models of the interaction of Alix with wild-type Gag-p6, Gag-p6Ser487A or phosphorylated Gag-p6-Ser487. Bottom panel shows structural models of the interaction of Vpr with wild-type Gag-p6, Gag-p6Ser487A or phosphorylated Gag-p6-Ser487. Binding energies of p6 with Alix or Vpr calculated from the structural models were shown in the bottom tables, where the highly negative value indicates the stable binding.

any effect on the interaction between Vpr and Gag. We have selected Bimolecular Fluorescence Complementation (BiFC) system to quantify the Vpr-Gag interaction in live cells as previously reported [34]. Plasmids encoding C-terminally KGC-tagged Gag (Gag-KGC) and N-terminally KGN-tagged Vpr (KGN-Vpr) were transfected and evaluated for BiFC signal by flow cytometry (Figure 5A). Flow cytometry analysis revealed that the interaction of Vpr with Gag-Ser487Ala mutant was reduced as compared with wild-type Gag (Figure 5A). To further assess whether the phosphorylation of Gag at Ser487 provides another hydrogen bond with Vpr Gln44 to facilitate Gag-

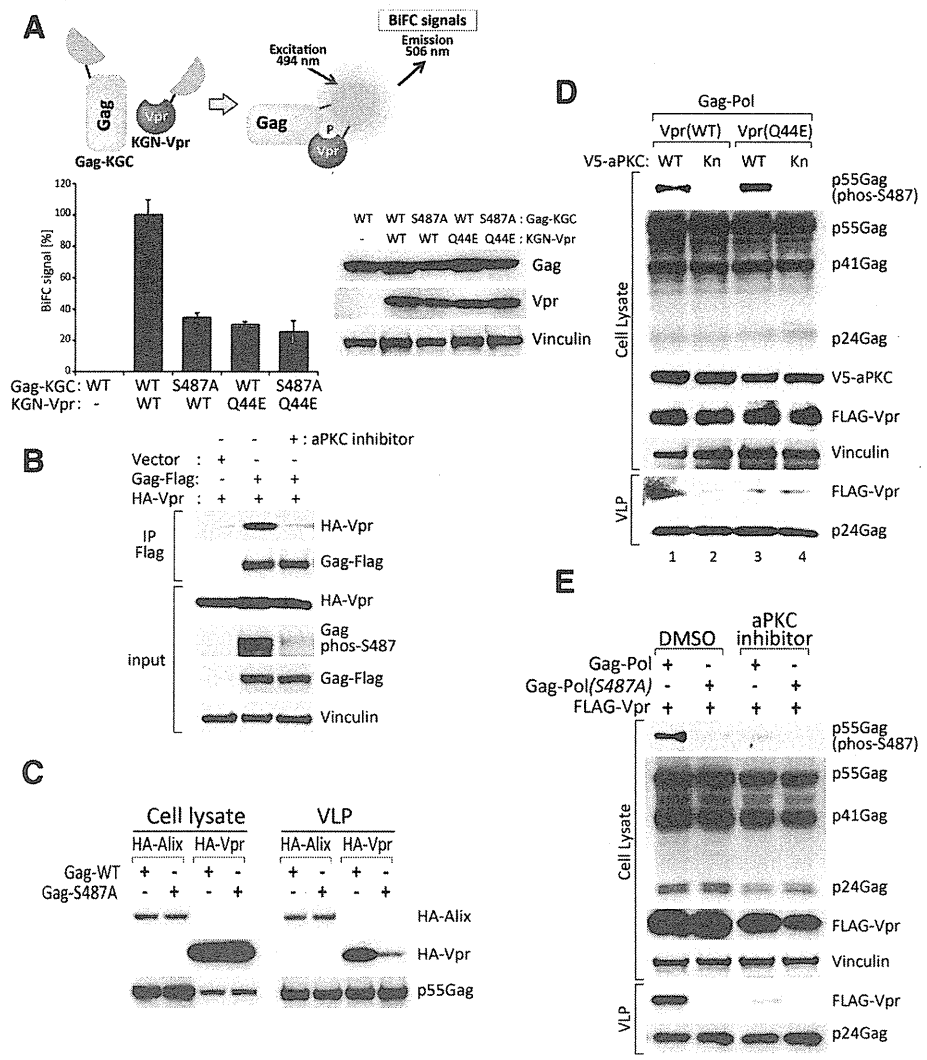

Figure 5 The phosphorylation of Gag at Ser487 promotes the incorporation of Vpr into HIV-1 virions. (A) Bimolecular fluorescence complementation (BiFC) of 293T cells expressing Gag-KGC and KGN-Vpr (upper panel). 293T cells were transfected with KGN-Vpr (WT or Q44E) and Gag-KGC or Gag (S487A)-KGC, were harvested and analyzed by flow cytometry to determine the BiFC signal at 48 hours post-transfection. Results represent the means of three independent experiments. The cells were harvested and subjected to western blot analysis. **(B)** The phosphorylation of Gag at Ser487 promotes interaction of Vpr with Gag. HA-tagged Vpr was co-transfected with Flag tagged Gag into 293T cells in presence of 5 μM aPKC inhibitor or DMSO, followed by pulldown with Flag-beads and immunoblotting with indicated antibodies. Bottom panel shows input for pulldown assay. **(C)** Differential effect of Gag Ser487 phosphorylation on Alix and Vpr incorporation into VLPs. 293T cells were transfected with GFP-tagged Gag (Gag-WT) or with the Ser487 point mutated Gag (Gag-S487A), with either HA-tagged Alix, or HA-tagged Vpr expression vectors. Cells and VLPs were collected at 24 hours post-transfection, and their protein extracts were resolved using SDS-PAGE and subjected to western blot analysis. **(D)** aPKC-mediated Gag phosphorylation at Ser487 facilitates Vpr incorporation into virions. 293T cells were transiently transfected with Gag-Pol, either Flag-tagged Vpr (WT) or Gln44 point mutated Vpr (Q44E), and with either V5-tagged aPKC (WT) or kinase-negative aPKC (Kn). Cell lysates and VLPs were collected 24 hours post-transfection and subjected to western blot analysis. **(E)** The phosphorylation of Gag-pol-Ser487 is required for Vpr incorporation into HIV-1 virions. 293T cells were transfected with Flag-tagged Vpr and either with Gag-Pol (WT) or with the Ser487 point mutated Gag-Pol (S487A). The transfected 293T cells were treated with DMSO or aPKC inhibitor for 24 hours. Cell lysates and VLPs were collected and subjected to western blot analysis.

Vpr interaction, we constructed Vpr Q44E mutant for BiFC analysis. Results demonstrated that Vpr Q44E mutant exhibited weker interactions to Gag and Gag S487A as compared with wild type Vpr (Figure 5A). We further found that aPKC inhibitor suppressed the interaction between Gag-Flag and HA-Vpr in imunoprecipitation analysis (Figure 5B).

The phosphorylation of Gag at Ser487 affects Vpr incorporation into virions and viral infectivity

We next examined whether the phosphorylation of Gag at Ser487 has any effects on the incorporation of Vpr into HIV-1 virus like particles (VLP). As shown in Figure 4B, we found no distinct changes in the incorporation of Alix into VLPs regardless of a Ser/Ala substitution at Gag Ser487 in 293T cells. However, Vpr incorporation into VLP was significantly decreased in cells transfected with the Gag-Ser487Ala mutant as compared with cells transfected with wild-type Gag (Figure 5C). Hence, it is plausible that the phosphorylation of Gag at Ser487 may have an important role in its interaction with Vpr thereby affecting the Vpr incorporation into VLPs.

To further explore the relevance of Gag phosphorylation to HIV-1 replication, we examined whether aPKC kinase activity is necessary to regulate Vpr incorporation into HIV-1 virions. Gag phosphorylation at Ser487 was prominently enhanced by wild type aPKC but not kinase negative mutant aPKC (Kn) (Figure 5D). Concomitantly, the level of Vpr incorporation into virions was shown to be paralleled with the Gag phosphorylation status (lane 1 and 2 in Figure 5D). More importantly, virion incorporation of Vpr Q44E mutant was much lesser than wild-type Vpr irrespective of Gag phosphorylation at Ser487 (lane3 and 4 in Figure 5D). These results suggest that Gag phosphorylation at Ser487 is indeed affect Vpr incorporation and this process could be mediated by the Gln44 residue of Vpr. Although no significant effect of the Gag-pol S487A mutant on the Vpr expression levels in cells was evident, the Vpr incorporation level into VLPs was significantly reduced upon Gag-pol-S487Ala transfection (Figure 5E). Consistent with this result, the incorporation of Vpr into VLPs was significantly reduced in cells treated with the aPKC inhibitor peptide; the Vpr incorporation efficiency was reduced in aPKC inhibitor treated cells (Figure 5E). These data indicate that aPKC can enhance the incorporation of Vpr into HIV-1 virions.

It has been well established that Vpr incorporation into HIV-1 virions augments viral infectivity in macrophages [5,6,35-37]. We thus assessed whether aPKC affects HIV-1 infectivity by increasing Vpr incorporation into virions. We hypothesized that if the Gag phosphorylation at Ser487 by aPKC was beneficial for HIV-1 infection in this way, aPKC activity would affect wild type HIV-1 but not a Vpr-null virus. To test this, we employed pNL4-3ΔEnv-luc (WT) or pNL4-3ΔEnvΔVpr-luc (Vpr-null) strains. We then produced the corresponding viruses with a fusiogenic envelope G glycoprotein of the vesicular stomatitis virus (VSV-G) in the presence or absence of aPKC inhibitor in 293T cells (Figure 6A). Immunoblotting analysis of VLP demonstrated that the level of Vpr incorporation was prominently reduced by treatment with the aPKC peptide inhibitor (Figure 6B). The infectivity of the generated viruses was tested using the human monocyte/macrophage cell line MonoMac6. The aPKC inhibitor-treated WT virus exhibited approximately 50% less infectivity than the control WT virus (Figure 6C). The Vpr-null virus showed a 35% reduction in infectivity compared with the WT virus in the MonoMac6 cells (Figure 6C). However, the primarily low infectivity of the Vpr-null virus was not significantly affected by the aPKC inhibitor (Figure 6C). aPKC inhibitor did not exhibit obvious cytotoxic effect to MonoMac 6 cells (Figure 6D).

To assess the role of aPKC in multi-round HIV-1 replication in primary monocyte-derived macrophages (MDMs), we infected these cells with HIV-$1_{89.6}$, a dual tropic virus, or HIV-1_{NLAD8}, an R5 tropic virus, in conjunction with treatments of various concentrations of the aPKC inhibitor (Figure 7A). The results revealed that the aPKC inhibitor strongly suppressed the replication of both viruses in a dose-dependent manner (Figure 7B, C), although there was no obvious toxicity or growth inhibition in these cells (Figure 7D). Taken together, these results indicate that the phosphorylation of Gag by aPKC regulates Vpr incorporation and HIV-1 replication in macrophages.

Discussion

We here demonstrate that aPKC is a crucial regulator of HIV-1 infection via the phosphorylation of Gag-p6 which enhances the incorporation of Vpr into virions. Our current data strongly suggest that Ser487 is the specific phosphorylation site on HIV-1 Gag for aPKC and is crucial for the Gag p6-Vpr interaction that leads to Vpr incorporation into viral particles. Furthermore, our current data demonstrate that an aPKC inhibitor prominently inhibits HIV-1 replication in primary human macrophages. Hence, the phosphorylation of Gag by aPKC may well be an important mechanism through which HIV-1 efficiently infects macrophages and by which an excessive accumulation of the cytotoxic Vpr protein in the host infected cells is prevented.

The Gag-p6 domain has been identified as the predominant site of phosphorylation in HIV-1 particles [22]. Ser487 is a highly conserved residue in this p6 domain among various HIV-1 strains, suggesting that the phosphorylation of this residue is of fundamental functional importance. Votteler et al. have demonstrated that a HIV-1 Gag mutant with a deleted PTAP region

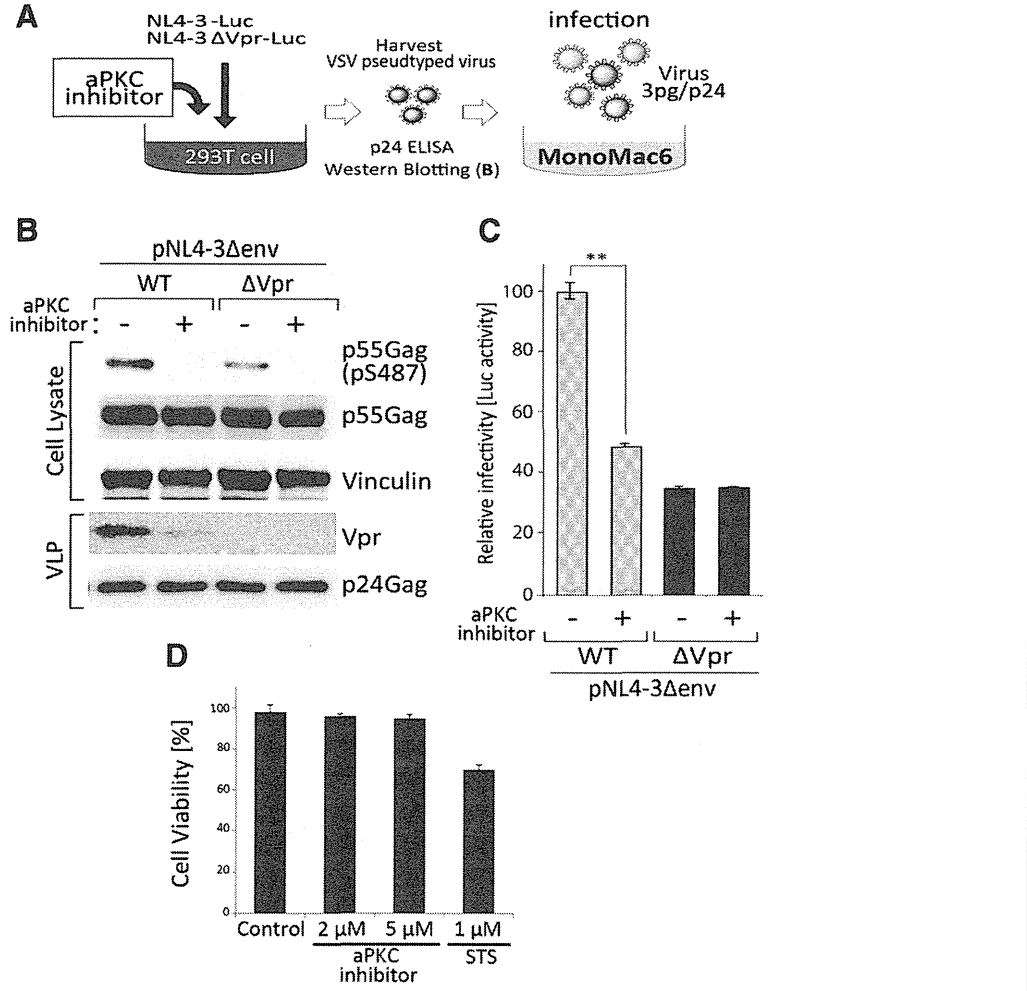

Figure 6 The inhibition of aPKC significantly decreases single-round HIV-1 infection. (A) Schematic representation of the experimental system. Briefly, 293T cells were either mock treated, or treated with aPKC inhibitor. After 4 hours, these cells were co-transfected with pNL4-3Δenv-luc or pNL4-3ΔenvΔVpr-luc and with pVSV-G. Viral release was measured through the quantification of p24CA antigen concentration in the culture supernatants at 48 hours post-transfection. MonoMac6 cells were infected with VSV-G pseudotyped WT and ΔVpr viruses for 48 hours. **(B)** The VSV-G pseudotyped WT and ΔVpr stocks generated from pNL4-3Δenv-luc and pNL4-3ΔenvΔVpr-luc with/without aPKC inhibitor treatment were analyzed by immunoblotting for the incorporation of Vpr into virion particles. **(C)** Viral infectivity was detected by measuring the luciferase activity in the cell lysates. Data are mean ± s.e.m. of three independent experiments. **(D)** Effects of aPKC inhibitors on viability of MonoMac6 cells. MonoMac6 cells were treated with aPKC inhibitor (2 or 5 μM) or 1 μM Staurosporine (STS) and analyzed for cell viability using trypan blue exclusion at 72 hours. Data are mean ± s.e.m. of three independent experiments: **$p < 0.01$, Student's t-test.

and a phenylalanine substitution at Ser487 (ΔPTAP/S487F) shows aberrant core formation and reduced viral infectivity in TZM-b1 cells [33]. More recently, steady state affinity analysis using a surface plasmon resonance sensorgram has revealed that the phosphorylated form of p6 at Ser487 has a stable binding affinity for cytoplasmic membranes [38]. These reports have therefore revealed that Gag Ser487 is a highly conserved phosphorylation site of likely crucial importance for HIV-1 infection. On the other hand, Radestock et al. recently reported in tissue culture experiments that the phosphorylation of Gag-p6 including Ser487 is dispensable for HIV-1 infectivity. These authors showed that asparagine substitutions at five serine residues (Ser487, Ser490, Ser494, Ser497 and Ser498) within the C-terminus of Gag p6 produced no impairment of Gag assembly or virus release and caused only very subtle deficiencies in viral infectivity in T-cell lines and in primary lymphocytes [39]. These discrepancies may be due to different experimental approaches using different Gag substitution mutants as well as different cell types. In contrast, our present approach is distinct from these earlier studies as we initially attempted to identify the kinases responsible for Gag-p6 phosphorylation and then explore their role in HIV-1 replication. Our current results clearly demonstrate that aPKC phosphorylates Gag-p6 and regulates the interaction of Gag with Vpr for

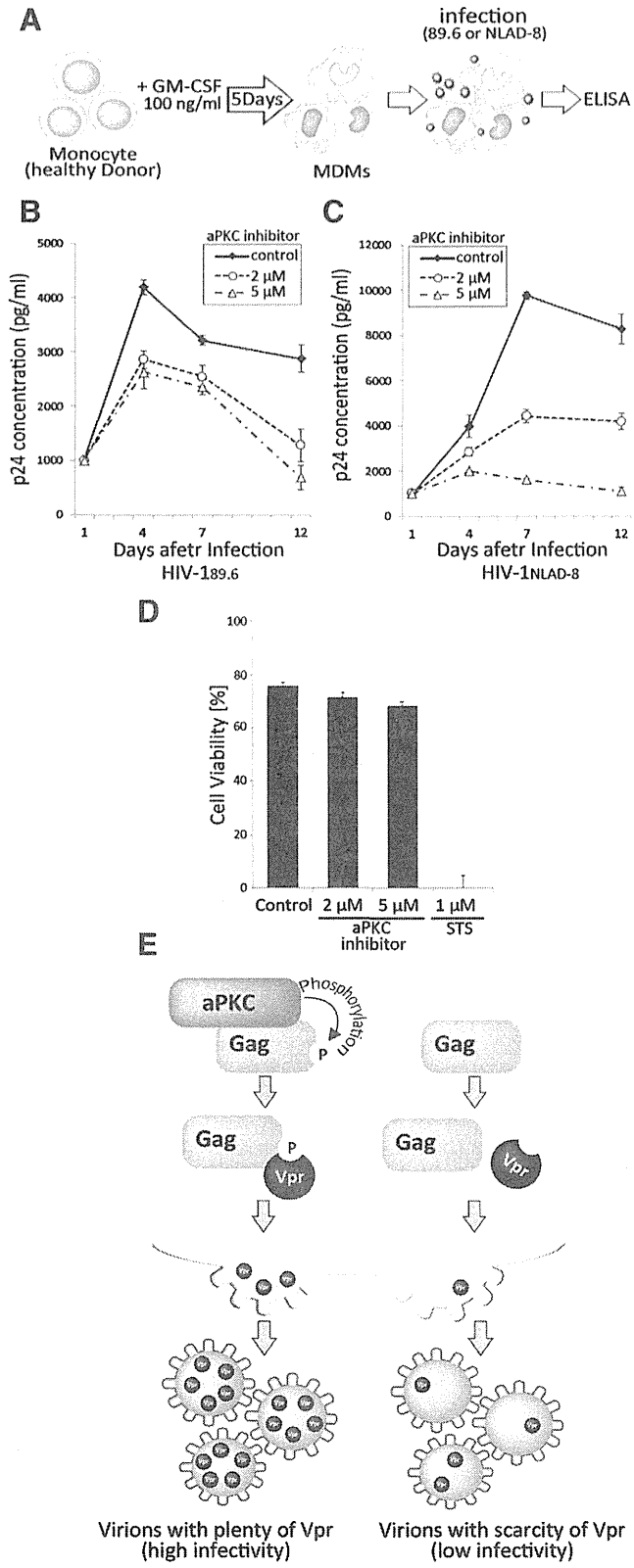

Figure 7 (See legend on next page.)

(See figure on previous page.)
Figure 7 The inhibition of aPKC significantly reduces replication competent HIV-1 infection. (A) Schema of the experimental system using HIV-1 replication competent HIV-$1_{89.6}$ and HIV-1_{NLAD-8}. Monocytes were isolated from buffy coat from healthy blood donors by positive selection on Monocyte Enrichment Cocktail and density gradient centrifugation as described in Methods. MDMs were generated by culturing monocytes with 100 ng/ml granulocyte-macrophage colony-stimulation factor for 5 days before HIV-1 infection. MDMs were infected with 5 ng of p24 from **(B)** HIV-$1_{89.6}$ or **(C)** HIV-1_{NLAD-8} virus and the levels of p24 capsid released into media during viral replication were assayed over a period of 12 days post infection. Data are the mean ± s.e.m. of three independent experiments: $^{**}P < 0.01$, Student's t-test. **(D)** Effects of aPKC inhibitor on viability of MDMs. MDMs cells were treated with aPKC inhibitor (2 or 5 μM) or 1 μM Staurosporine (STS) and analysed for cell viability using trypan blue exclusion at 96 hours. **(E)** Schematic model of our current study. aPKC phosphorylate HIV-1 Gag at Ser487. This phosphorylation promotes the interaction between Gag and Vpr, thereby facilitating viral infectivity in macrophages.

the incorporation of Vpr into virus particles. These specific effects of aPKC-mediated Gag-p6 phosphorylation are consistent with the evidence that the substitution of Gag Ser487 for Ala significantly decreases Vpr incorporation and viral infectivity. On the other hand, inhibition of aPKC in cells may have other additional effects on HIV-1 replication cycle rather than Gag phosphorylation for the Vpr incorporation. To observe the specific effect of aPKC on Gag phosphorylation, we created Gag and Vpr mutants devoid of the effect of aPKC and these mutants were less competent in virus replication. However, aPKC may regulate other cellular function directing HIV replication. Although our current data clearly demonstrate a crucial role of aPKC in Gag Ser487 phosphorylation and interaction Gag-Vpr to Vpr incorporation, further detailed analyses may be necessary to clarify the molecular signature of Gag p6 phosphorylation on multiple stages of the HIV-1 replication cycle.

We show from our current experiments that Gag Ser487 phosphorylation has a significant impact on p6-Vpr binding. Vpr is a non-structural viral protein that is incorporated into virions and possesses several characteristic features and functions that are known to play important roles in HIV-1 replication and disease progression [40]. The presence of a functional Vpr in viral particles is necessary for the efficient translocation of the pre-integration complex (PIC) into the nucleus and subsequent infection of primary monocytes/macrophages and other non-dividing cells [5,6]. Vpr also has a crucial role in viral replication, apoptosis, cell cycle arrest and in the down-regulation of immune activation [37,41-43]. Many Vpr functions are carried out by virion-associated Vpr [44], suggesting that the incorporation of Vpr into virus particles is an important event not only in HIV-1 replication but also in HIV-1 mediated cytopathogenesis.

Several previous reports have indicated that p6 is phosphorylated during HIV-1 infection [2,22]. However, these studies did not undertake any detailed investigation of the biological significance of this phosphorylation event through biochemical or structural analyses. Our current computer-assisted structural modeling and AlphaScreen homogenous proximity assays have revealed that the phosphorylated Gag at Ser487 binds more stably to Vpr whereas there was no significant difference in the interaction of Gag-p6 with Alix, consistent with previous reports [31,32]. The phosphorylation of Ser487 can create another hydrogen bond between Gag-Ser487 and Vpr-Gln44. In consistent with this data a previous study indicated that the site specific deletion of Gln44 resulted in the significant reduction of Vpr incorporation into virions [34]. We also demonstrate that Gag phosphorylation at Ser487 affects Vpr incorporation and this process could be mediated by Gln44 residue of Vpr.

We show in our current study that Gag phosphorylation on Ser487 itself does not affect the binding affinity of Gag with Alix. However, resultant Vpr interaction to Gag may hinder the Alix-Gag interaction at the LYPXnL motif. This may eliminate Alix from nascent VLP and impeded its ability to function in HIV-1 release in PTAP-deficient strains of HIV. On the other hands, Alix also interacts with the nucleocapsid (NC) domain of HIV-1 Gag in addition to binding the LYPXnL motif [45], there by linking Gag to components of ESCRT-III. Therefore, further analysis is needed to fully understand the molecular link between Gag phosphorylation and virus release through the Alix/LYPXnL pathway.

We further explored the physiological significance of Vpr incorporation into virions. Our current results clearly demonstrate that the inhibition of aPKC-mediated Vpr incorporation prominently reduces the viral infectivity in MDMs. These results together indicate that Gag phosphorylation by aPKC plays a crucial role in the HIV-1 infection of macrophages.

aPKC has been demonstrated to be involved in cell polarity and migration in a number of study models [46]. During cell migration, aPKC localizes on the leading edge of the plasma membrane where HIV-1 Gag is also localized in infected cells. It has been reported in an earlier study that aPKC is located at an immunological synapse with potential importance in cell-to-cell viral transfer [47]. It is thus plausible that aPKC may regulate the incorporation of Vpr into virions at the leading edges or the HIV-1 virological synapse in polarized cells [48]. It would be interesting to investigate whether aPKC cooperates with other factors in polarized HIV-1-infected cells in an additional mechanism to its function in Gag phosphorylation.

In the earlier study by Folgueira et al. [49], it was demonstrated that aPKC mediates the NF-κB transcriptional activation required for HIV-1 infection in U937 cells. It is of particular interest that aPKC is a one of the key regulators of HIV-1 infection. Our present findings also provide evidence for the involvement of aPKC in HIV-1 replication by showing that it directly phosphorylates Gag on Ser487, and that this phosphorylation mediates Vpr incorporation into virions. The targeting of aPKC activity is therefore a potential option as a novel therapeutic intervention against HIV-1 infection in combination with existing anti-retroviral treatments.

Conclusions

We have identified aPKC as a host protein kinase that phosphorylates HIV-1 Gag at its Ser487 residue. Computer assisted structural modeling and subsequent biochemical assays revealed that the phosphorylation of Gag Ser487 enhances the association of Gag with Vpr and promotes the resultant incorporation of Vpr into virions. These events facilitate viral infectivity in macrophages. Hence, aPKC inhibition is a potential new therapeutic approach against HIV-1 infection in human macrophages.

Methods

Viral DNA constructs and plasmids

The HIV-1 reporter virus vectors pNL4-3ΔEnv-Luc and pNL4-3ΔEnvΔVpr-Luc were provided by Akifumi Takaori-Kondo (Kyoto University, Kyoto, Japan) [50,51]. The HIV-1 recombinant molecular clone pHIV-$1_{89.6}$ and pHIV-1_{NLAD8} were provided by Akio Adachi (Tokushima University, Tokushima, Japan). The HIV-1 Gag and HIV-1 p6 (pNL4-3) derived-DNA fragment was generated by PCR and inserted into the pEU-E01-GST-MCS vector (Cellfree Sciences, Yokohama, Japan). Using this subcloned plasmid, we generated substitution mutants with PrimSTAR Max (Takara Bio Inc, Shiga, Japan) and the following primers for Ser487A,

5'-TTAACTGCGCTCAGATCACTCTTTGGC-3' and 5'-TCTGAGCGCAGTTAAAGGATACAGTTC-3'. Plasmids expressing HIV-1 Gag-Pol were provided by Jun Komano [52] (National Institute of Infectious Diseases, Tokyo, Japan). Expression vectors encoding aPKCλ wt and aPKCλ kn, a kinase-deficient mutant, have been previously described [53]. C-terminal Flag-tagged p55Gag (codon-optimized) has been previously described [54]. All the DNA experiments were approved by Gene and Recombination Experiment Safety Committee at the Yokohama City University School of Medicine.

Antibodies and other reagents

The anti-p24 (CA) mouse monoclonal antibody (clone Kal-1) was purchased from Dako (Glostrup, Denmark). Anti-Flag (M2) and anti-Vinculin mouse monoclonal antibodies were obtained from Sigma (St. Louis, MO). Anti-PKCι mouse monoclonal antibody was from BD transduction (Franklin Lakes, NJ). Polyclonal rabbit anti-Vpr antibody was obtained from the AIDS research and Reference Reagent Program, National Institute of Allergy and Infectious Diseases (US National Institute of Health, Germantown, MD). The peptide specific antibody against PLT (pS) LRSLFGND (phosphorylated at Ser487 of Gag peptide from 484 to 495) was generated by Scrum Inc (Tokyo, Japan). The myristoylated (myr) PKC ζ peptide inhibitor myr-PKCζ (N-myr-Ser-Ile-Tyr-Arg-Arg-Gly-Ala-Arg-Arg-Trp-Arg-Lys-Leu-OH) and myr-PKC α and β (N-myr-Phe-Ala-Arg-Lys-Gly-Ala-Leu-Arg-Gln-NH_2) were purchased from Merck (Darmstadt, Germany). Akt inhibitor was obtained from Calbiochem (Darmstadt, Germany), and the PI3K inhibitor Wortmannin was obtained from Merck. The Cdk inhibitor roscovitine was purchased from Promega (Madison, WI). All inhibitors were dissolved in DMSO and stocks were aliquoted and stored at −60°C until use. The final concentration of each inhibitor used is indicated in the figure legends.

Cells and viruses

Monocytes were isolated from buffy coat from healthy blood donors by positive selection on Monocyte Enrichment Cocktail (Stemcell, Tukwila, WA) and Lymphoprep (Stemcell) density gradient centrifugation with SepMate-50 (Stemcell). MDMs were generated by culturing monocytes with 100 ng/ml granulocyte-macrophage colony-stimulation factor for 5 days. 293T and HeLa cells were cultured in DMEM (Gibco-BRL, Rockville, MD) supplemented with 10% (V/V) fetal bovine serum (FBS) (Gibco-BRL). HIV-$1_{89.6}$ and HIV-1_{NLAD-8} strains were produced in 293T cells. Vesicular stomatitis virus G glycoprotein (VSV-G)-pseudotyped viruses were produced in 293T cells cotransfected with reporter virus plasmid and VSV-G using the calcium-phosphate method. The culture supernatants were collected and subjected to quantification of HIV-1 particle yields by p24CA antigen capture enzyme-linked immunosorbent assay (ELISA) (Zepto Metrix, Buffalo, NY). Monocyte isolation and treatment were approved by the Ethics Committee at the Yokohama City University School of Medicine.

In vitro protein production

A total of 287 cDNAs encoding human protein kinases were constructed as described previously [23]. The protein production method has also been described previously [55-57]. Briefly, DNA templates containing a biotin-ligating sequence were amplified by split-PCR using cDNAs and corresponding primers, and then used with the Gen-Decoder protein production system (Cell Free Science, Ehime, Japan). For HIV-1 Gag protein synthesis, *Gag* genes derived from the pNL4-3 proviral plasmid [58] were